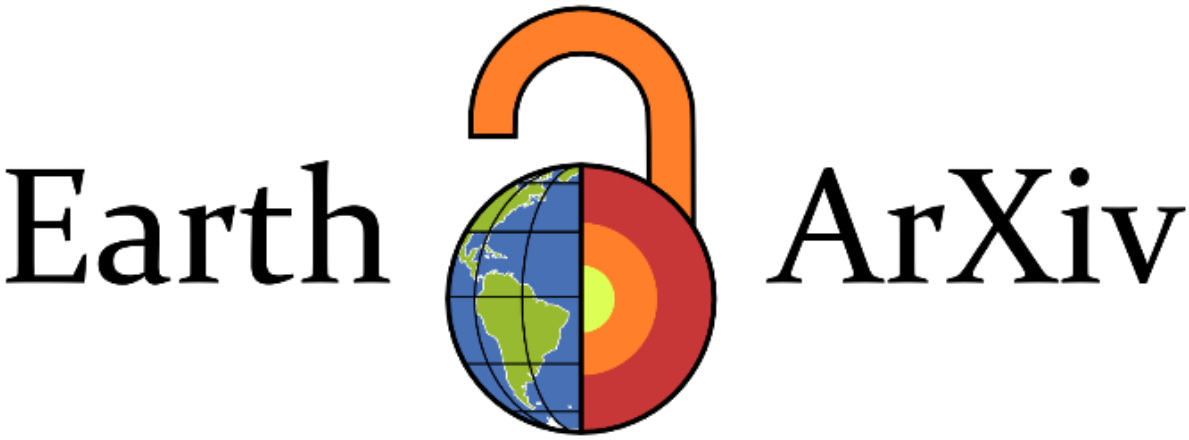

A response surface framework for persistence-aware lime requirement

Authors and affiliations

Hamza Jouichat[a,1], Lotfi Khiari[a,*,2]

[a] Department of Soil Science and Agrifood Engineering, Laval University, Québec, QC, Canada.

[1] ORCID: 0000-0003-4957-2854.

[2] ORCID: 0000-0003-3793-1186.

[*] Corresponding author: lotfi.khiari@fsaa.ulaval.ca.

Abstract

Conventional lime-requirement (LR) methods estimate the dose needed to attain a target soil pH, but do not indicate how long the correction remains acceptable during re-acidification. We tested whether repeated dose–response measurements could provide a persistence-aware LR. Single applications of calcium carbonate ($CaCO_3$) and calcium oxide (CaO) were evaluated in clay, sandy loam, and organic soils over five 12-week cropping cycles. Each cycle included ryegrass growth, fertilisation, and three harvests; pH was measured at the end of each cycle. Response surfaces described how the pH response changed during continued cropping. We defined the peak lime requirement, LR_{peak}, as the smallest dose whose highest fitted pH across C1–C5 attained the target; peak therefore denotes the maximum fitted response, not the duration of the pH correction. We defined the persistence-aware lime requirement, $LR_{\mathrm{freq}}(N)$, as the dose that remained within selected pH bounds and closest to the target over N cycles. We also defined the persistence ratio, $r(N)$, as $LR_{\mathrm{freq}}(N)$ divided by LR_{peak}; it expresses the persistence-aware rate relative to the peak target-attainment rate. Under $CaCO_3$, pH at LR_{peak} fell below the lower agronomic bound in the second cycle in all three soils. For a proposed persistence horizon, the surface first tests whether any dose remains within both bounds through every cycle; when feasible, $LR_{\mathrm{freq}}(N)$ selects the rate closest to the target. Under $CaCO_3$, $LR_{\mathrm{freq}}(5)$ was feasible for clay and organic soil. Sandy loam had no five-cycle strict-bound solution; its longest feasible

horizon was two cycles, for which $LR_{\mathrm{freq}}(2)$ was selected. At each soil's longest feasible horizon, LR_{freq} (t ha^{-1}) was 5.00 for clay, 4.15 for sandy loam, and 7.72 for organic soil; corresponding $r(N)$ values were 1.66, 1.14, and 1.36. Over the corresponding horizons, predictions at LR_{freq} had mean squared deviations from target pH 84.0%, 32.4%, and 75.7% lower than predictions at LR_{peak} for clay, sandy loam, and organic soil, respectively. The response surfaces therefore show how lime rate, the selected pH limits, and the intended number of cycles interact. When one dose can remain within both limits, LR_{freq} identifies the rate that stays closest to the target.

Keywords

Soil acidity; Lime requirement; Soil pH buffering; Re-acidification; Lime persistence; Mitscherlich model

1. Introduction

Soil acidity constrains crop production through its effects on nutrient availability, aluminium and manganese solubility, microbial activity, and root growth (Fageria and Baligar, 2008; Neina, 2019; Barrow and Hartemink, 2023). Liming can correct acidity, but that correction is not permanent. Ammonium-based fertilisation, removal of base cations in harvested biomass, and leaching continue to generate or export acidity after lime application (Helyar and Porter, 1989; Edmeades and Ridley, 2003; Tang and Rengel, 2003; Ghimire et al., 2017; Hao et al., 2020). The agronomic value of a lime rate therefore depends on two outcomes: how far it initially raises pH and how long the resulting correction persists.

Lime requirement (LR) is conventionally expressed as the mass of liming material needed to raise soil pH to a specified target (McLean, 1982). The reference incubation approach estimates this quantity by equilibrating a soil with a series of lime additions and identifying the dose at which the endpoint response reaches the target. Operational buffer methods, including Shoemaker–McLean–Pratt (SMP) and Mehlich procedures, provide faster LR estimates by calibrating the soil–buffer pH response against LR values obtained from reference incubation tests at specified target-pH endpoints (Shoemaker et al., 1961; Mehlich, 1976; Tran and van

Lierop, 1982; van Lierop, 1983). Their calibration therefore preserves the incubation method's endpoint definition: the dose required to attain target pH. Because neither the calibration endpoint nor the routine buffer measurement includes repeated observation of re-acidification, these methods cannot by themselves determine how long pH will remain acceptable or when lime should be reapplied. In practice, rate is obtained from soil testing, whereas reapplication timing is commonly managed through periodic retesting and regional guidance (CRAAQ, 2010; Goulding, 2016; OMAFRA, 2022).

Although routine LR methods treat rate and reapplication timing separately, previous dynamic models have shown that the two decisions can be considered jointly. Lukin and Epplin (2003) modelled pH change under continuous wheat production to optimise application amount and timing, while Xu et al. (2022) combined soil buffering and acid-production balances to estimate regional lime requirements and intervals. Long-term experiments likewise show that residual lime effects and re-acidification differ among soils and management systems (Holland et al., 2019). These studies establish the importance of the rate–interval relationship, but they do not derive a bounded rate recommendation directly from repeated experimental dose–response curves. Addressing that gap requires following the same lime-dose series through successive cropping periods.

Building a common representation from these repeated observations requires a consistent mathematical description of the dose response at each cycle. Lime–pH curves are non-linear: successive increments of lime produce progressively smaller pH gains as the response approaches an asymptote. The Mitscherlich equation provides a compact description of this pattern and has a long history in agricultural dose–response analysis (Mitscherlich, 1909; Spillman, 1923; Dhanoa et al., 2022; Jouichat and Khiari, 2026). Linking Mitscherlich descriptions of successive cycle-specific responses could therefore extend the endpoint LR concept from a single dose–response curve to a response surface.

The premise of such a surface is that liming rate and persistence are linked. Larger applications may leave more residual neutralising capacity and a greater pH margin before a selected lower threshold is reached, thereby extending the interval over which liming remains effective (Edmeades and Ridley, 2003; Goulding, 2016). This potential benefit is constrained by the agronomic risks of excessive pH, including reduced availability of Fe, Mn, Zn, B, and P (Bolan

et al., 2003; Curtin and Trolove, 2013; Penn and Camberato, 2019). Because the acceptable interval lies between lower and upper pH limits, application rate and reapplication interval cannot be selected independently. The interval between these limits can be viewed as an agronomic pH window, whose appropriate width and position depend on the crop, soil, and management context. For some soils or intended horizons, no single application may remain within the selected window throughout the entire period.

We hypothesised that a response surface could model the rate–frequency relationship by linking a selected rate to its persistence within the agronomic pH window and a selected horizon to the rate that best maintains target pH. We further expected this persistence-aware LR to produce smaller deviations from target than the peak LR, which identifies target attainment at the highest fitted response but imposes no persistence requirement.

Accordingly, this study aimed to (i) construct response surfaces for three contrasting acidic soils; (ii) evaluate how closely the fitted responses reproduced measured pH and whether a curve-based analysis and parametric surface gave similar LR estimates; (iii) use the fitted responses to estimate $LR_{freq}(N)$, $r(N)$, and the first fitted cycle in which pH was below the lower limit at each dose; and (iv) examine how the resulting rate–frequency relationship varied among soils and between $CaCO_3$ and CaO.

2. Materials and methods

2.1 Soil selection, preparation, and characterisation

Three acidic soils from Quebec, Canada (eastern North America), were selected to represent contrasting matrices: a clay mineral soil, a sandy loam, and an organic soil. The soils were air-dried and passed through a 4 mm sieve before potting. Their baseline properties are reported in Table 1.

Soil pH in water (pH_{water}) was measured at a 1:1 soil-to-water ratio (v/v) for the mineral soils and 1:4 for the organic soil because of its greater water absorption (van Lierop, 1981; Parent and Tremblay, 2002). Buffer pH (pH_{SMP}) was measured at a 1:1:2 soil:water:SMP-buffer ratio using 10 mL soil, 10 mL deionised water, and 20 mL buffer (Shoemaker et al., 1961). The soil–water suspension was agitated for 30 min at 180 cycles min^{-1}; buffer was then added, the mixture was

stirred manually for 15 min, and pH_{SMP} was recorded. Organic matter was determined by the Walkley–Black method (Walkley and Black, 1934; Nelson and Sommers, 1982), and mineral-soil particle-size distribution by the hydrometer method (Day, 1965). Mehlich-3-extractable bases and trace elements were analysed by inductively coupled plasma spectroscopy (Mehlich, 1984). Cation exchange capacity and base saturation were determined by ammonium acetate extraction at pH 7 (Lavkulich, 1981); exchangeable acidity ($H^+ + Al^{3+}$) was determined by KCl extraction and titration (Thomas, 1982).

Table 1. Baseline physicochemical properties of the three soils.

Property	Clay	Sandy loam	Organic
Clay (%)	57.3	5.2	8.6
OM (%)	2.4	3.4	62.8
pH_{water}	5.60	4.61	4.18
pH_{SMP}	5.93	5.60	4.62
CEC ($cmol_c\ kg^{-1}$)	12.4	2.3	13.4
Exch. Al ($cmol_c\ kg^{-1}$)	0.0	1.7	4.3
Exch. acidity ($cmol_c\ kg^{-1}$)	0.03	1.95	7.44
BS (%)	99.8	16.8	44.4

Note: Clay (%) = clay fraction of mineral material; OM = soil organic matter; pH_{water} = pre-treatment soil pH at 1:1 (soil:water) for the mineral soils and 1:4 for the organic soil; pH_{SMP} = SMP-buffer pH (Shoemaker–McLean–Pratt); CEC = cation exchange capacity; Exch. Al = exchangeable Al by KCl extraction and titration; Exch. acidity = exchangeable Al + H by KCl extraction and titration; BS = base saturation.

2.2 Greenhouse design and liming treatments

The greenhouse experiment comprised soil- and product-specific dose series rather than a fully crossed common-dose design. Calcium carbonate ($CaCO_3$) and calcium oxide (CaO) were applied to each soil at 7–10 dose levels (Table 2), with one pot per soil × product × dose treatment. The same pot was followed through five successive 12-week cropping cycles; each cycle comprised fertilisation, three ryegrass harvests, and a pH measurement at the end of the cycle, as detailed in Section 2.3. $CaCO_3$ was the reference material. Pure CaO has a neutralising value of approximately 179 relative to $CaCO_3$ = 100; CaO doses were therefore converted to $CaCO_3$-equivalent rates for comparisons between materials. Table 2 distinguishes the actual CaO

mass applied from its $CaCO_3$-equivalent rate. Both liming materials were analytical grade (≥99% purity) and ground to pass a 250 µm sieve.

The plastic pots used were slightly conical and had perforated, geotextile-lined bases, a surface area of 0.013 m², and a depth of 10.19 cm. Pots received 1.0 kg clay, 1.1 kg sandy loam, or 0.4 kg organic soil. Lime was applied once, before the first cycle, and mixed into the upper half of the soil column. No lime was added during subsequent cycles.

Table 2. Experimental design.

Soil	Pot mass (kg)	Dose levels per product	$CaCO_3$ range (t ha^{-1})	CaO range, actual (t ha^{-1})	Cycles
Clay	1.00	7	0.0–12.0	0–6.72	5
Sandy loam	1.10	9	0.0–18.0	0–10.08	5
Organic	0.40	10	0.0–21.0	0–11.76	5

Note: $CaCO_3$ rates are both actual-product and $CaCO_3$-equivalent rates. CaO rates were converted using a stoichiometric neutralising-value factor of 1.785. Lime was applied once before C1; the same pots were then followed through five successive 12-week cycles.

2.3 Crop management, sampling, and measurements

Fifty annual ryegrass seeds (*Lolium multiflorum* L. var. Maris Ledger) were sown uniformly in each pot. Ryegrass was selected because it tolerates acidic conditions, regrows after cutting, and supports repeated nutrient removal under sustained N fertilisation (Wilman, 1975; Meharg and Killham, 1990; Gastal and Lemaire, 2015). Greenhouse temperature was maintained at 18–22 °C and relative humidity at 60% under a 14 h photoperiod at 1–200 µmol m^{-2} s^{-1}. Pots were irrigated daily while avoiding drainage sufficient to cause appreciable nutrient loss.

Each cycle lasted approximately 12 weeks and began with ryegrass sowing and the fertilisation programme in Table 3. The rates in Table 3 are total nutrient amounts per cycle; these totals were distributed among the initial liquid application and reapplications after each ryegrass cut to sustain plant nutrition and re-impose the acidifying load. Shoots were harvested when heading was visible in more than 5% of pots, approximately 6, 9, and 12 weeks after sowing. At the end of each cycle, soil was sampled immediately after the third harvest, and pH was measured on the dried samples using the soil-to-water ratios described in Section 2.1. The sequence was repeated for five cycles, yielding five pH measurements (one at the end of each cycle) and 15 biomass observations per pot. Shoot dry mass (DM, g pot^{-1}) was summed across the three harvests within

each cycle. Because removal of plant biomass exports base cations and can contribute to acidification, the dose–DM association was examined as a descriptive check on whether plant response varied systematically with lime dose.

Fertiliser rates followed Quebec agronomic guidance (CRAAQ, 2010). The sandy loam received more N and K than the other soils (Table 3), so soil type and fertilisation intensity were not separable in comparisons of re-acidification among soils.

Table 3. Fertilisation programme per 12-week cycle.

Nutrient source	Clay	Sandy loam	Organic
N (kg ha^{-1})	120	150	120
P_2O_5 (kg ha^{-1})	60	60	–
K_2O (kg ha^{-1})	120	240	120
N sources	MAP + $(NH_4)_2SO_4$	MAP + $(NH_4)_2SO_4$	KNO_3 + $(NH_4)_2SO_4$
P source	MAP	MAP	–
K source	K_2SO_4	K_2SO_4	K_2SO_4

Note: Values are total nutrient rates per cycle, distributed among the initial application and the post-cut reapplications. Fertiliser source grades follow the convention N-P_2O_5-K_2O (percent by mass). MAP = monoammonium phosphate.

2.4 Response surface construction

The pH response was modelled in two steps. First, a dose–response curve was fitted independently within each cropping cycle. Second, these five fitted curves were analysed directly and were also summarised by a continuous parametric surface.

Let i index the fitted cycle and $H = 5$ denote the number of fitted cycles. For each soil, all dose-based calculations were confined to $\mathcal{D} = [0, D^{\max}_{\text{tested}}]$, the continuous $CaCO_3$-equivalent dose interval from zero to the largest dose tested. The upper limits were 12, 18, and 21 $t\ ha^{-1}$ for clay, sandy loam, and organic soil, respectively. Within each cycle, the lime-induced pH response was defined relative to the corresponding unlimed control:

$$\Delta pH_i(D) = \widehat{pH}_i(D) - pH_{0,i}$$

Here, $\widehat{pH}_i(D)$ is the predicted soil pH at dose D in cycle i, and $pH_{0,i}$ is the observed pH of the corresponding unlimed control.

The Mitscherlich model was fitted to ΔpH so that the unlimed control represented background acidification under cropping and fertilisation, while the fitted response represented the additional pH increase attributable to lime. This separation prevents the downward drift of the control from being attributed to changes in the lime-response parameters. In this parameterisation, A_i is the fitted maximum pH increase above the unlimed control in cycle i, approached as dose increases, and c_i controls the curvature of that response across dose.

For the mineral soils, $\Delta pH_i(D)$ was modelled using a Mitscherlich-type equation:

$$\Delta pH_i(D) = A_i(1 - e^{-c_i D}) \qquad (1)$$

For the organic soil, the low-dose treatments showed an extended low-response region, so a threshold dose $D_{0,i}$ was included:

$$\Delta pH_i(D) = \begin{cases} 0, & D \leq D_{0,i} \\ A_i\{1 - e^{-c_i(D - D_{0,i})}\}, & D > D_{0,i} \end{cases} \qquad (2)$$

Here, $D_{0,i}$ is the fitted dose threshold below which the model assigns no lime-induced pH increase. Standard errors for A_i and c_i, and for $D_{0,i}$ in the organic soil, were obtained from the non-linear least-squares covariance matrix. They indicate how precisely each parameter was determined by the dose response within that cycle.

$CaCO_3$ was the primary material used to compare two temporal representations; CaO was analysed in the same way after conversion to a $CaCO_3$-equivalent dose. The *curve-based analysis* retained the five independently fitted Mitscherlich curves. It therefore imposed no function on the evolution of the fitted parameters across cycles. The *parametric surface* instead represented each Mitscherlich parameter as a continuous function of cycle. For graphical presentation, the five cycle-specific curves were displayed as a curve-based contour surface. Shape-preserving piecewise cubic Hermite interpolation (PCHIP) was applied across cycle number to pH_0, A and c values for the mineral soils and additionally to D_0 for the organic soil.

For the parametric surface, each cycle-dependent Mitscherlich parameter was represented by one of four candidate functions. For each soil, $f(t)$ stood for $A(t)$, $c(t)$, or, for the organic soil, $D_0(t)$ where t represent the temporal component (cycles). The candidates were $f(t) = \beta_0$, $f(t) = \beta_0 + \beta_1 t$, $f(t) = \beta_0 + \beta_1 t + \beta_2 t^2$, and $f(t) = \beta_\infty + (\beta_0 - \beta_\infty)e^{-\lambda t}$. The coefficients

were fitted separately for each parameter and soil; in the exponential form, β_∞ is the plateau and λ controls the approach to it across cycles.

Each combination of candidate functions was substituted into the Mitscherlich model and fitted by non-linear least squares directly to all observed ΔpH values across doses and cycles, with equal weight given to each observation. The cycle-specific parameter estimates and their standard errors were used to compare the independent curves with the fitted temporal functions in Fig. 3, but they were not used as observations or weights when fitting the parametric surface. The combination with the lowest Akaike information criterion corrected for small sample size (AICc) was selected for each soil (Burnham and Anderson, 2002; Archontoulis and Miguez, 2015). The resulting parametric model can be written as:

$$\Delta pH(D,t) = A(t)\left\{1 - e^{-c(t)\max[0,D-D_0(t)]}\right\} \qquad (3)$$

In Eq. (3), $D_0(t) = 0$ for the mineral soils, whereas the organic-soil threshold followed its selected cycle function; the maximum operator enforces zero lime response below that threshold. Absolute pH was recovered using the cycle-specific control defined above. PCHIP connected the observed control values only for continuous display between cycles, and the control trajectory was not included in AICc selection.

For both materials, the curve-based analysis supplied the primary operational estimates because it used the five fitted cycle responses without temporal smoothing. The parametric surface tested whether replacing those independent responses with a smoother, lower-dimensional representation changed predictive agreement or the derived rates.

2.5 Response-derived rate–frequency metrics

To derive the rate–frequency outputs, both analyses were evaluated within a selected agronomic pH window. The window was an operational input used to demonstrate the modelling strategy, not a fitted parameter or a universal tolerance range. Quebec guidance gives an adequate range of pH 6.0–7.0 for forage grasses in mineral soils and a general target range of pH 5.0–5.8 for organic soils (CRAAQ, 2010). Within the mineral-soil range, pH 6.3 was adopted as the lower bound because soils above this value are typically treated as not requiring lime application; the target and upper bound were 6.5 and 7.0, respectively. For organic soil, the lower bound, target, and upper bound were 5.0, 5.4, and 6.0, respectively and window width was expressed as $\delta =$

$pH_{\text{upper}} - pH_{\text{lower}}$. *Strict-bound* required pH to remain at or above the lower bound through the selected horizon and at or below the upper bound at every fitted cycle C1–C5.

The following metrics translated the fitted responses into a joint assessment of application rate and persistence.

For a chosen period of N consecutive cycles after liming (the persistence horizon), $D_{\min}(N)$ was defined as the smallest dose predicted to keep pH at or above the lower acceptable limit in every one of those cycles:

$$D_{\min}(N) = \min_{D \in \mathcal{D}} D \quad \text{subject to} \quad \widehat{pH}(D, t) \geq pH_{\text{lower}} \quad \text{for every } t = 1, \dots, N \qquad (4)$$

To prevent excessive liming, $D_{\max}$ was defined as the largest dose predicted to remain at or below the upper acceptable pH limit in every fitted cycle from C1 to C5:

$$D_{\max} = \max_{D \in \mathcal{D}} D \quad \text{subject to} \quad \widehat{pH}(D, t) \leq pH_{\text{upper}} \quad \text{for every } t = 1, \dots, H \qquad (5)$$

If no dose within $\mathcal{D}$ kept pH above the lower limit for all N cycles, $D_{\min}(N)$ did not exist for that period. If no dose within $\mathcal{D}$ reached the upper limit, $D_{\max}$ was set to $D_{\text{tested}}^{\max}$. When $D_{\min}(N) \leq D_{\max}$, every dose between them satisfied both pH limits. This interval, termed the feasible dose corridor, was

$$\mathcal{F}(N) = [D_{\min}(N), D_{\max}] \qquad (6)$$

The interval was non-empty only when $D_{\min}(N) \leq D_{\max}$; otherwise, no single dose could satisfy both pH limits for all N cycles. $N_{\max}$ was defined as the greatest number of consecutive cycles for which at least one such dose existed:

$$N_{\max} = \max_{N \in \{1, \dots, H\}} N \quad \text{subject to} \quad D_{\min}(N) \leq D_{\max} \qquad (7)$$

If no single dose kept pH within both limits throughout all N cycles, the selected N-cycle period was classified as infeasible. The fitted trajectories could then be used to compare a shorter period, revised pH limits, or doses associated with small departures from either limit. For each dose, we also recorded the first fitted cycle endpoint at which pH was below the lower limit. If pH remained at or above the lower limit at every endpoint from C1 to C5, we recorded no crossing through C5.

The peak lime requirement, LR_{peak}, was defined as the smallest dose whose highest fitted pH across C1–C5 attained the target:

$$LR_{peak} = \min_{D \in \mathcal{D}} D \quad \text{subject to} \quad \max_{t \in \{1,\ldots,H\}} \widehat{pH}(D,t) \geq pH_{\text{target}} \qquad (8)$$

Here, *peak* refers to the highest fitted pH across the observed cycles, it is conceptually analogous to LR traditionally derived from incubation response curves (Kouera and Khiari, 2026) because both identify a dose that attains target pH, but LR_{peak} was calculated from the fitted greenhouse responses and extends over the 5 cycle curves.

Within an open feasible set, a contrasting persistence-aware lime requirement was defined as:

$$LR_{freq}(N) = \arg\min_{D \in \mathcal{F}(N)} \frac{1}{N} \sum_{t=1}^{N} \left[\widehat{pH}(D,t) - pH_{\text{target}}\right]^2 \qquad (9)$$

If $\mathcal{F}(N)$ is empty, $LR_{freq}(N)$ is undefined under the selected strict window.

The ratio between the persistence-aware and peak requirements was computed as:

$$r(N) = \frac{LR_{freq}(N)}{LR_{peak}} \qquad (10)$$

The ratio $r(N)$ was treated as a descriptive measure of the difference between the peak and persistence-aware rates. Its transfer to independently measured incubation LR requires paired calibration. When $LR_{\text{freq}}(N)$ is undefined, $r(N)$ is also undefined for that horizon.

Target tracking for any dose D over N cycles was quantified as the mean squared deviation from the soil-specific target pH:

$$MSD(D,N) = \frac{1}{N} \sum_{t=1}^{N} \left[\widehat{pH}(D,t) - pH_{\text{target}}\right]^2 \qquad (11)$$

$MSD(D,N)$ is the average squared distance between fitted and target pH over cycles 1 through N. We set $MSD_{\text{peak}} = MSD(LR_{\text{peak}}, N)$ and $MSD_{\text{freq}} = MSD(LR_{\text{freq}}(N), N)$, using the same horizon for both rates. The percentage improvement in target tracking was:

$$\text{MSD reduction (\%)} = 100\,\frac{MSD_{\text{peak}} - MSD_{\text{freq}}}{MSD_{\text{peak}}} \qquad (12)$$

Positive values indicate a smaller average squared deviation from target pH at LR_{freq} than at LR_{peak}.

Before the experiment, lime requirement was estimated from each soil's SMP-buffer pH using the regional estimation grid of CRAAQ (2010). This estimate, denoted LR_{CRAAQ}, served as a benchmark for comparison with the experimentally derived LR values and as an anchor for selecting the experimental dose series; the maximum tested rate was set above LR_{CRAAQ}.

2.6 Model assessment and statistical analysis

The coefficient of determination (R^2) and root mean square error (RMSE) evaluated agreement of modeled curves and surfaces with the observed pH values. Both metrics were calculated by pooling predictions from the five cycle-specific curves and separately for the parametric surface. Operational stability was assessed by comparing N_{max}, LR_{peak}, LR_{freq}, and $r(N)$ between the curve-based analysis and the parametric surface.

As an ancillary analysis, cycle-specific dry mass was summarised across all $CaCO_3$ rates tested in each soil. Spearman's rank correlation coefficient (ρ) was calculated within each soil and cycle to describe the association between lime dose and DM.

Analyses were conducted in Python 3.10. Mitscherlich curves were fitted by non-linear least squares and PCHIP interpolation for graphical presentation used scipy. Numerical processing used numpy, scipy, pandas, and pyarrow, and figures were produced with matplotlib.

3. Results

3.1 Ryegrass dry-mass response

Across all dose and cycle combinations in the complete soil-specific $CaCO_3$ ranges, mean dry mass (DM) was 5.59 g pot^{-1} in clay, 5.97 g pot^{-1} in sandy loam, and 5.72 g pot^{-1} in organic soil.

Spearman correlations between $CaCO_3$ dose and DM ranged from -0.43 to $+0.14$ across clay cycles. All sandy-loam correlations were positive ($+0.23$ to $+0.55$). In organic soil, ρ increased from 0.84 at C1 to 0.95 at C5 (Table 4). CaO correlations spanned -0.29 to $+1.00$ in clay, -0.73 to -0.07 in sandy loam, and $+0.47$ to $+0.93$ in organic soil (Supplementary Table S1).

Table 4. Ryegrass dry mass and Spearman correlation with $CaCO_3$ application rate by soil and cycle.

Cycle	Soil	Mean DM ± SD (g pot^{-1})	CV (%)	ρ
1	Clay	5.40 ± 0.93	17.2	+0.00
1	Sandy loam	4.94 ± 1.14	23.0	+0.38
1	Organic	4.56 ± 1.52	33.4	+0.84
2	Clay	5.72 ± 0.59	10.3	−0.07
2	Sandy loam	6.12 ± 1.31	21.4	+0.53
2	Organic	4.97 ± 2.05	41.3	+0.87
3	Clay	5.94 ± 2.85	48.0	+0.14
3	Sandy loam	7.40 ± 1.07	14.5	+0.23
3	Organic	8.32 ± 1.71	20.5	+0.89
4	Clay	5.35 ± 0.48	8.9	−0.18
4	Sandy loam	5.80 ± 1.11	19.2	+0.48
4	Organic	5.22 ± 2.10	40.2	+0.94
5	Clay	5.53 ± 0.70	12.7	−0.43
5	Sandy loam	5.60 ± 1.09	19.5	+0.55
5	Organic	5.52 ± 1.90	34.5	+0.95

Note: DM = dry mass; SD = standard deviation; CV = coefficient of variation; ρ = Spearman correlation between applied $CaCO_3$ dose and per-cycle DM. DM is the per-pot sum of three harvests within each 12-week cycle. Mean ± SD, CV, and ρ were calculated across all tested $CaCO_3$ rates: seven rates for clay (0–12 t ha^{-1}), nine for sandy loam (0–18 t ha^{-1}), and ten for organic soil (0–21 t ha^{-1}).

3.2 pH trajectories and cycle-specific dose responses

The $CaCO_3$ trajectories showed a dose-dependent transition from brief correction to persistence (Fig. 1). In clay, 4 t ha^{-1} reached the target at C1, and 6–12 t ha^{-1} remained above it through

C5. In sandy loam, 6 t ha^{-1} remained above the target through C2, and 8–18 t ha^{-1} remained above it through C5. In organic soil, 8 t ha^{-1} reached the target at C1, and 10–21 t ha^{-1} remained above it through C5. Lower-dose treatments commonly reached their highest pH at C1 and declined over later cycles. Increasing dose reduced the post-C1 decline, and the highest-dose trajectories became comparatively stable across cycles.

Cycle-specific Mitscherlich fits closely reproduced the observed dose responses, with R^2 values of 0.939–0.989 and RMSE values of 0.10–0.31 pH units (Fig. 2). In the mineral soils, A increased and c declined across cycles (Fig. 3). Over the same period, the unlimed controls acidified, high-dose treatments maintained a larger pH advantage, and lower-to-intermediate doses retained progressively smaller corrections. Increasing A captured the widening fitted difference at high dose, while decreasing c captured the flatter response across lower and intermediate rates. Fit-derived standard errors were largest in organic soil, averaging 28% of A and 52% of c. They averaged 12% of A and 27% of c in clay, and 7% of A and 17% of c in sandy loam.

Clay showed approximately linear changes in both A and c. Sandy loam combined an approximately linear increase in A with a non-linear decrease in c. Organic-soil A varied little, and c declined towards a low plateau. The independently fitted organic-soil D_0 values were more variable across cycles (Fig. 2).

3.3 Parametric form selection and agreement with cycle-specific fits

AICc selected linear $A(t)$ and linear $c(t)$ for clay; linear $A(t)$ and quadratic $c(t)$ for sandy loam; and constant $A(t)$, exponential-plateau $c(t)$, and constant $D_0(t)$ for organic soil. The closest alternatives were 1.35, 0.57, and 2.57 AICc units above the selected combinations for clay, sandy loam, and organic soil, respectively (Fig. S2). These close rankings indicate appreciable functional-form uncertainty, and the selected equations provide parsimonious summaries of the observed temporal patterns.

Using these forms, the selected parametric $CaCO_3$ surfaces were:

For the clay soil:

$$\Delta pH(D,t) = (2.168 + 0.307t)\left\{1 - e^{-(0.299-0.032t)D}\right\} \qquad (13)$$

For the sandy loam soil:

$$\Delta pH(D,t) = (2.671 + 0.367t)\left\{1 - e^{-(0.419-0.128t+0.014t^2)D}\right\} \qquad (14)$$

For the organic soil:

$$\Delta pH(D,t) = 4.200\left\{1 - e^{-(0.071+0.347e^{-1.985t})\max(0,D-2.831)}\right\} \qquad (15)$$

Coefficients in Eqs. (13)–(15) are rounded to three decimals for presentation; all calculations and figures use the full-precision fitted coefficients.

Both $CaCO_3$ analyses closely reproduced the observed pH values (Fig. 4). For clay, sandy loam, and organic soil, the pooled cycle-specific curves gave R^2 values of 0.968, 0.972, and 0.962 and RMSE values of 0.178, 0.207, and 0.224 pH units, respectively. The parametric surfaces gave R^2 values of 0.954, 0.969, and 0.951 and RMSE values of 0.212, 0.221, and 0.255 pH units. With 4–5 coefficients per soil, the parametric surfaces retained the principal pH patterns represented by 10–15 coefficients in the cycle-specific curves.

3.4 Rate–frequency estimates and comparison with traditional LR estimation.

The curve-based analysis and parametric surface gave similar persistence-aware rates (Fig. 5; Table 5). Curve-based LR_{freq} values were 5.00, 4.15, and 7.72 t ha^{-1} for clay, sandy loam, and organic soil, respectively. Corresponding parametric values were 4.97, 4.42, and 7.70 t ha^{-1}. Absolute differences were 0.03, 0.27, and 0.02 t ha^{-1}. These small differences indicate limited sensitivity of LR_{freq} to temporal smoothing.

Both analyses gave $N_{\max} = 5$ for clay and organic soil and $N_{\max} = 2$ for sandy loam. In sandy loam, $D_{\min}(5)$ exceeded $D_{\max}$: 6.91 versus 5.93 t ha^{-1} for the cycle-specific curves and 6.75 versus 5.98 t ha^{-1} for the parametric surface. Thus, MSD comparisons covered C1–C5 for clay and organic soil and C1–C2 for sandy loam. Fig. 5 places the target, operational pH bounds, and $LR_{\mathrm{freq}}(N_{\max})$ on both pH landscapes.

Over these soil-specific horizons, LR_{freq} exceeded LR_{peak} in every soil. Relative to LR_{peak}, curve-based LR_{freq} reduced MSD from target pH by 84.0% in clay, 32.4% in sandy loam, and 75.7% in organic soil. The corresponding parametric-surface reductions were 64.7%, 31.1%, and 69.5%. Between the curve-based and parametric analyses, LR_{peak} differed by 0.68 t ha^{-1} in clay

and 0.82 t ha^{-1} in organic soil. These differences yielded $r(N_{max})$ values of 1.66 versus 1.34 in clay and 1.36 versus 1.18 in organic soil.

The LR_{CRAAQ} were 10.0, 13.4, and 16.1 t ha^{-1} for clay, sandy loam, and organic soil. Each exceeded the fitted D_{max} under the selected greenhouse pH windows. Showing that the regional recommendations largely overestimated LR.

Table 5. $CaCO_3$ rate–frequency and peak-response metrics from the curve-based analysis and parametric surface.

Metric	Clay		Sandy loam		Organic	
	Curve-based	Parametric	Curve-based	Parametric	Curve-based	Parametric
LR_{CRAAQ}	10.00	10.00	13.40	13.40	16.10	16.10
N_{max}	5	5	2	2	5	5
LR_{peak}	3.02	3.70	3.63	3.70	5.68	6.50
$LR_{freq}(N_{max})$	5.00	4.97	4.15	4.42	7.72	7.70
$r(N_{max})$	1.66	1.34	1.14	1.20	1.36	1.18
$D_{min}(5)$	4.99	4.97	6.91	6.75	7.17	6.78
D_{max}	5.90	6.03	5.93	5.98	8.41	8.65
MSD reduction (%)	84.0	64.7	32.4	31.1	75.7	69.5

Note: Rates are expressed as t $CaCO_3$ ha^{-1}. LR_{CRAAQ} is the regional SMP-buffer estimate made before the experiment. N_{max} is the greatest number of consecutive cycles for which at least one dose remained between the lower and upper pH limits. LR_{peak} is the smallest dose whose highest fitted pH across C1–C5 reached the target. $LR_{freq}(N_{max})$ is the feasible dose with the smallest mean squared deviation (MSD) from target pH over that horizon. $r(N_{max}) = LR_{freq}(N_{max})/LR_{peak}$. $D_{min}(5)$ is the smallest dose that remained at or above the lower pH limit through C5. D_{max} is the largest dose that remained at or below the upper pH limit throughout C1–C5. MSD reduction is the percentage decrease in MSD from target pH at LR_{freq} relative to LR_{peak}, using N_{max} for both rates (Eqs. 11 and 12).

3.5 CaO response at matched neutralising value

The AICc-selected CaO parametric surfaces used constant $A(t)$ and $c(t)$ for clay; linear $A(t)$ and exponential-plateau $c(t)$ for sandy loam; and constant $A(t)$, exponential-plateau $c(t)$, and constant $D_0(t)$ for organic soil (Table S3). Their observed-data R^2 values were 0.928–0.943 and RMSE values were 0.226–0.297 pH units. The nearest alternatives were 0.38, 0.37, and 0.99 AICc units above the selected clay, sandy-loam, and organic-soil forms, respectively.

At matched $CaCO_3$-equivalent loadings, both analyses required higher LR_{freq} values for CaO than for $CaCO_3$ in every soil. In the curve-based analysis, the respective CaO and $CaCO_3$ values were 6.47 versus 5.00 t ha^{-1} in clay at N = 5, 5.58 versus 4.15 t ha^{-1} in sandy loam at N = 2, and 9.89 versus 7.72 t ha^{-1} in organic soil at N = 5. On the parametric surfaces, they were 6.22 versus 4.97, 6.07 versus 4.42, and 9.47 versus 7.70 t ha^{-1} at the same soil-specific horizons. Both analyses also retained $N_{max} = 5$, 2, and 5 for clay, sandy loam, and organic soil. The material ranking was therefore insensitive to temporal smoothing.

Parametric and curve-based CaO LR_{freq} differed by 0.25 t ha^{-1} in clay, 0.49 t ha^{-1} in sandy loam, and 0.42 t ha^{-1} in organic soil. Curve-based CaO LR_{peak} values were 4.76, 5.03, and 7.71 t ha^{-1}, and parametric values were 5.61, 4.86, and 7.98 t ha^{-1}. The corresponding curve-based $r(N_{\mathrm{max}})$ values were 1.36, 1.11, and 1.28; parametric values were 1.11, 1.25, and 1.19. Both analyses also selected higher $CaCO_3$-equivalent LR_{peak} values for CaO than for $CaCO_3$ in all three soils. Tables S2 and S3 report the CaO LR metrics and selected parametric functions, and Fig. S1 shows both temporal representations.

4. Discussion

4.1 From target attainment to persistence

Traditional incubation and calibrated buffer methods estimate the lime rate required to attain a selected target pH (Shoemaker et al., 1961; Mehlich, 1976; McLean, 1982; Tran and van Lierop, 1982; van Lierop, 1983). In the present experiment, LR_{peak} achieved the target pH during the first cropping cycle (C1) in all three soils, yet pH fell below the lower acceptable threshold by C2. A rate sufficient to reach the target initially was therefore not necessarily sufficient to maintain an acceptable pH over time. Reformulating the modelling objective from attaining the target at a single time point to maintaining pH as close as possible to the target, while remaining within predefined bounds over a specified period, identified LR_{freq} as the more appropriate rate for sustained pH management. This distinction highlights that lime recommendations should account not only for the rate needed to reach the target pH, but also for the period over which acceptable pH is expected to be maintained.

Previous studies have linked lime rate and application interval through economic optimisation

under continuous cropping (Lukin and Epplin, 2003) or through regional calculations combining soil buffering capacity with acid-production balances (Xu et al., 2022). The present approach complements these frameworks by deriving the rate–frequency relationship directly from repeated experimental pH responses. The response surface links each lime rate to the number of cycles for which fitted pH remains within the selected range. This adds information about pH persistence that can guide pH monitoring and reapplication planning.

4.2 Interpreting persistence and reapplication

Differences in $N_{\max}$ among soils indicate that appropriate reapplication schedules may vary with soil and management conditions. This agrees with long-term studies showing soil-specific differences in the persistence of liming effects (Holland et al., 2019). However, $N_{\max}$ alone provides an incomplete basis for reapplication decisions because its strict criterion treats any excursion outside the selected limits as a loss of feasibility, regardless of its magnitude, duration, or subsequent recovery. The complete response surface provides the additional information needed to distinguish among these trajectories and evaluate the practical consequences of accepting a small excursion.

Fig. 6 illustrates this distinction for sandy loam. Under the selected pH limits, sandy loam had $N_{\max} = 2$. Alternatively, $D_{\min}(5)$ =6.91 t ha^{-1} maintained pH at or above the lower limit throughout all five cycles while exceeding the upper limit by only 0.13 pH unit at C1. Predicted pH remained within both limits from C2 to C5. The surface therefore allows practitioners to compare continuous compliance over two cycles with a management option that accepts a small, temporary upper-limit excursion in exchange for longer pH persistence. This trajectory-level information provides a more complete basis for comparing lime rates and planning pH monitoring than $N_{\max}$ alone.

The response surface makes this trade-off visible. It supports comparison among continuous compliance over a shorter period, longer persistence with a small quantified departure, and revised pH limits. Crop sensitivity, micronutrient status, and the consequences of low and high pH determine which option is appropriate (Bolan et al., 2003; Curtin and Trolove, 2013; Penn and Camberato, 2019). Reapplication planning should therefore combine the fitted trajectory with current pH measurements and local agronomic conditions.

Fig. 7 shows the first fitted cycle in which pH was below the lower limit for each dose. An earlier crossing identifies doses for which pH may need to be checked sooner. Fig. 6 shows the size and duration of each departure and whether pH later returned within the selected range. A reapplication decision also requires a current soil pH measurement and consideration of the crop and management conditions.

4.3 Role of the selected pH limits

The selected pH limits define the amount of deviation that is considered agronomically acceptable. A narrow range leaves fewer suitable rates and may shorten $N_{\max}$, while a wider range permits more rate and persistence combinations. Fig. 8 shows that the availability of a five-cycle rate depends strongly on this choice, especially in sandy loam. The limits should therefore reflect crop sensitivity, soil properties, and management priorities (CRAAQ, 2010), with the calculations applying those agronomic choices.

Widening the pH range can move LR_{freq} upward or downward because both the lower and upper constraints are relaxed. At the first feasible window width, the available rate may lie on either side of the dose that best tracks target pH. As the range widens, LR_{freq} moves towards that target-tracking dose and then stabilises. Feasibility therefore describes a specific combination of soil response, persistence period, and accepted pH limits. Reporting the limits and testing their influence are essential when interpreting a surface-derived rate.

4.4 Effects of soil and liming material

In the mineral soils, the greater persistence observed at high $CaCO_3$ rates is consistent with residual neutralising material continuing to react as acidity accumulated during later cycles (Edmeades and Ridley, 2003; Goulding, 2016). The difference in persistence between clay and sandy loam further suggests that application rate acted together with soil buffering and fertilisation intensity. Measurements of residual carbonate, exchangeable acidity, and base saturation across cycles would help distinguish the contribution of these processes.

Sandy loam had the lowest clay content, organic matter, and cation-exchange capacity, all of which contribute to pH buffering (Magdoff and Bartlett, 1985; Curtin and Rostad, 1997; Curtin and Trolove, 2013). It also received the highest N and K inputs. Nitrification of ammonium can accelerate acidification (Helyar and Porter, 1989; Hao et al., 2020). Weak buffering and greater

fertilisation intensity provide a plausible joint explanation for the rapid rise above the upper limit followed by the sharper decline towards the lower limit. Such soils may require more frequent lime reapplications than buffered soils.

The organic soil required the highest five-cycle rate, and its high-dose pH remained comparatively stable after C1. Organic matter provides substantial pH-dependent charge and buffering through carboxyl and phenolic groups (Helling et al., 1964; Curtin and Rostad, 1997; Sebastià et al., 2008), while peat responses to liming vary with decomposition and application rate (Prasad et al., 2021). These properties can explain the observed combination of a large initial lime requirement and sustained correction at high rates. The dry-matter response to lime likewise depended on initial soil acidity. The association between $CaCO_3$ rate and dry mass was strongest in the organic soil (ρ = 0.84–0.95), which had the lowest pH and highest exchangeable acidity and Al (Table 1), weaker but consistently positive in the sandy loam (ρ = 0.23–0.55), and absent in the clay (ρ = −0.43 to +0.14), where initial pH was 5.60 and exchangeable Al was 0.0 cmolc kg^{-1}. This pattern agrees with Hillard et al. (1992), who reported large ryegrass yield gains from liming a strongly acidic Ultisol (pH 4.7), attributing the response primarily to Al toxicity and limited P, Ca, and Mg availability rather than to low pH alone.

At matched neutralising value, CaO required higher $CaCO_3$-equivalent LR_{peak} and LR_{freq} values than $CaCO_3$ in all three soils. This result was contrary to the expectation that faster-reacting CaO would provide an equal or greater pH correction (Getahun et al., 2021). Because pH was measured at the end of each 12-week cycle, these results describe the correction remaining after the early reaction period. Earlier measurements would clarify the initial CaO response. Material type, particle size, and application method can influence pH response beyond nominal neutralising value (Calva and Espinosa, 2017; Li et al., 2019; Makaza et al., 2026). Persistence should therefore be calibrated separately for each liming material.

4.5 Limitations and future calibration

One pot represented each soil × product × dose treatment. The fitted curves, AICc rankings, biomass associations, and derived LR values describe those experimental units. Replicated experiments are needed to estimate variation among pots and test treatment effects. Replication would also reduce the influence of individual observations on cycle-specific curves, especially at low doses. The comparison between the curve-based and parametric analyses measures

numerical stability within this dataset. Independent observations are needed to evaluate predictive performance.

The experiment included one soil per class, one crop, and one controlled greenhouse acidification regime. Sandy-loam properties and its higher fertilisation rate occurred together, so its persistence results describe that combined system. A factorial design would separate soil and fertilisation effects. Field calibration should also include uneven lime placement, seasonal temperature and rainfall, and base-cation leaching, which influence residual lime response (Cregan et al., 1989; Edmeades and Ridley, 2003; Goulding, 2016). Field evidence is also required to relate the controlled 12-week cycles to calendar reapplication intervals.

The observed $r(N_{\max})$ values ranged from 1.14 to 1.66. The sandy-loam value describes two cycles, whereas the clay and organic-soil values describe five cycles; each value is therefore specific to a soil and persistence horizon. Because repeated multi-dose experiments require substantial time, greenhouse space, crop management, and laboratory analysis, their practical use will require a staged development pathway. At the simplest level, an average $r(N)$ established for a defined soil–management group and number of cycles could multiply routine incubation LR as a persistence correction coefficient. Estimating a transferable average will require replicated multi-soil data.

With a larger calibration dataset, a more refined approach could predict $r(N)$ from soil properties, acidifying inputs, liming material, and the intended number of cycles. Routine buffer methods illustrate this calibration strategy: equations linking SMP and Mehlich buffer values to incubation-derived LR were developed for specified soil groups and target pH values (Shoemaker et al., 1961; Mehlich, 1976; Tran and van Lierop, 1982; van Lierop, 1983). Multi-cycle experiments could similarly provide reference $r(N)$ values for calibration. The predicted ratio could then adjust routine incubation LR to estimate $LR_{freq}(N)$ before liming.

With sufficiently broad multi-cycle data, a third approach could predict the complete sequence of lime-response curves or the response surface itself. Jouichat and Khiari (2026) reconstructed complete soil acidity-neutralisation curves from routine chemical or mid-infrared spectral information. Extending that strategy across repeated cycles could predict a complete pH response surface for a new soil. The predicted surface could then estimate $LR_{freq}(N)$, $N_{\max}$, and pH over

time for a proposed rate. This approach requires more data than calibration of a single ratio, but it retains the timing and magnitude of departures from the selected pH limits.

The close agreement in LR_{freq} between the curve-based and parametric analyses indicates numerical stability of the persistence-aware rate within this dataset. The larger between-analysis differences in LR_{peak} show that $r(N)$ calibration requires a consistent analysis. Future calibration should use standardised procedures and report prediction uncertainty. Field trials can then relate experimental cycles to management time and evaluate the predicted rates under different fertilisation, weather, lime-incorporation, and reapplication strategies.

5. Conclusions

This study demonstrates that attaining target pH at the peak response does not ensure sustained correction during continued acidification. Predicted pH at LR_{peak} fell below the lower limit in later cycles, whereas response surfaces fitted across repeated cropping cycles and evaluated against selected pH limits identified LR_{freq}, the rate that maintained pH closest to target over a defined period. LR_{freq} consistently exceeded LR_{peak} and reduced deviation from target pH by 31.1–84.0%. These findings show that response surfaces provide a more complete basis for LR formulation by distinguishing peak target attainment from persistence. Differences in $N_{\max}$ and trajectory shape showed that rate, persistence, and accepted pH limits must be interpreted together. Complete trajectories supplied the timing and magnitude needed to interpret a single feasibility classification. The ratio $r(N)$ summarises the additional rate associated with persistence and provides a practical quantity for future calibration. By adding persistence to classical endpoint LR estimation, the framework connects lime-rate selection with the expected duration of pH correction, monitoring, and reapplication planning.

CRediT author statement

Hamza Jouichat: Conceptualization, Methodology, Software, Formal analysis, Investigation, Data curation, Visualization, Writing — original draft. **Lotfi Khiari:** Conceptualization, Methodology, Resources, Supervision, Funding acquisition, Project administration, Writing — review & editing.

Declaration of competing interest

The authors declare that they have no known competing financial interests or personal relationships that could have appeared to influence the work reported in this paper.

Acknowledgments

This work was conducted within the DAQARA project, supported by NSERC and four industrial partners: Rio Tinto, Graymont, Omya, and OCP-Africa.

Data and code availability

The data used for this study is confidential.

Supplementary material

Supplementary material associated with this article is provided in a separate file and comprises Tables S1–S3 and Figs S1–S2. Table S1 reports the CaO biomass results, Table S2 reports CaO lime-requirement metrics from both analyses, and Table S3 gives the selected CaO parametric functions and fit metrics. Fig. S1 shows the curve-based and parametric CaO response surfaces, and Fig. S2 summarises parametric model selection for $CaCO_3$.

References

Archontoulis, S.V., Miguez, F.E., 2015. Nonlinear regression models and applications in agricultural research. Agron. J. 107, 786–798. https://doi.org/10.2134/agronj2012.0506

Barrow, N.J., Hartemink, A.E., 2023. The effects of pH on nutrient availability depend on both soils and plants. Plant Soil 487, 21–37. https://doi.org/10.1007/s11104-023-05960-5

Bolan, N.S., Adriano, D.C., Curtin, D., 2003. Soil acidification and liming interactions with nutrient and heavy metal transformation and bioavailability. Adv. Agron. 78, 215–272. https://doi.org/10.1016/S0065-2113(02)78006-1

Burnham, K.P., Anderson, D.R., 2002. Model Selection and Multimodel Inference: A Practical Information-Theoretic Approach, 2nd ed. Springer, New York. https://doi.org/10.1007/b97636

Calva, C., Espinosa, J., 2017. Efecto de la aplicación de cuatro materiales de encalado en control de la acidez de un suelo de Loreto, Orellana. Siembra 4, 110–120. https://doi.org/10.29166/siembra.v4i1.505

CRAAQ, 2010. Guide de référence en fertilisation, 2e éd. Centre de référence en agriculture et agroalimentaire du Québec, Québec, QC, 473 pp. ISBN 978-2-7649-0231-8.

Cregan, P.D., Hirth, J.R., Conyers, M.K., 1989. Amelioration of soil acidity by liming and other amendments, in: Robson, A.D. (Ed.), Soil Acidity and Plant Growth. Academic Press, Sydney, pp. 205–264. https://doi.org/10.1016/B978-0-12-590655-5.50011-6

Curtin, D., Rostad, H.P.W., 1997. Cation exchange and buffer potential of Saskatchewan soils estimated from texture, organic matter and pH. Can. J. Soil Sci. 77, 621–626. https://doi.org/10.4141/S97-015

Curtin, D., Trolove, S., 2013. Predicting pH buffering capacity of New Zealand soils from organic matter content and mineral characteristics. Soil Res. 51, 494–502. https://doi.org/10.1071/SR13137

Day, P.R., 1965. Particle fractionation and particle-size analysis, in: Black, C.A. (Ed.), Methods of Soil Analysis, Part 1: Physical and Mineralogical Properties, Including Statistics of Measurement and Sampling. Agronomy Monograph 9. American Society of Agronomy, Madison, WI, pp. 545–567. https://doi.org/10.2134/agronmonogr9.1.c43

Dhanoa, M.S., Sanderson, R., Cardenas, L.M., Shepherd, A., Chadwick, D.R., Powell, C.D., Ellis, J.L., López, S., France, J., 2022. Overview and application of the Mitscherlich equation and its extensions to estimate the soil nitrogen pool fraction associated with crop yield and nitrous oxide emission. Adv. Agron. 174, 269–295. https://doi.org/10.1016/bs.agron.2022.03.005

Edmeades, D.C., Ridley, A.M., 2003. Using lime to ameliorate topsoil and subsoil acidity, in: Rengel, Z. (Ed.), Handbook of Soil Acidity. Marcel Dekker, New York, pp. 297–336. https://doi.org/10.1201/9780203912317.ch11

Fageria, N.K., Baligar, V.C., 2008. Ameliorating soil acidity of tropical Oxisols by liming for sustainable crop production. Adv. Agron. 99, 345–399. https://doi.org/10.1016/S0065-2113(08)00407-0

Gastal, F., Lemaire, G., 2015. Defoliation, shoot plasticity, sward structure and herbage utilization in pasture: review of the underlying ecophysiological processes. Agriculture 5, 1146–1171. https://doi.org/10.3390/agriculture5041146

Getahun, G.T., Etana, A., Munkholm, L.J., Kirchmann, H., 2021. Liming with $CaCO_3$ or CaO affects aggregate stability and dissolved reactive phosphorus in a heavy clay subsoil. Soil Tillage Res. 214, 105162. https://doi.org/10.1016/j.still.2021.105162

Ghimire, R., Machado, S., Bista, P., 2017. Soil pH, soil organic matter, and crop yields in winter wheat–summer fallow systems. Agron. J. 109, 706–717. https://doi.org/10.2134/agronj2016.08.0462

Goulding, K.W.T., 2016. Soil acidification and the importance of liming agricultural soils with particular reference to the United Kingdom. Soil Use Manag. 32, 390–399. https://doi.org/10.1111/sum.12270

Hao, T., Zhu, Q., Zeng, M., Shen, J., Shi, X., Liu, X., Zhang, F., de Vries, W., 2020. Impacts of nitrogen fertilizer type and application rate on soil acidification rate under a wheat–maize double cropping system. J. Environ. Manage. 270, 110888. https://doi.org/10.1016/j.jenvman.2020.110888

Helling, C.S., Chesters, G., Corey, R.B., 1964. Contribution of organic matter and clay to soil cation-exchange capacity as affected by the pH of the saturating solution. Soil Sci. Soc. Am. J. 28, 517–520. https://doi.org/10.2136/sssaj1964.03615995002800040020x

Helyar, K.R., Porter, W.M., 1989. Soil acidification, its measurement and the processes involved, in: Robson, A.D. (Ed.), Soil Acidity and Plant Growth. Academic Press, Sydney, pp. 61–101. https://doi.org/10.1016/B978-0-12-590655-5.50007-4

Hillard, J.B., Haby, V.A., Hons, F.M., 1992. Annual ryegrass response to limestone and phosphorus on an Ultisol. J. Plant Nutr. 15, 1253–1268. https://doi.org/10.1080/01904169209364394

Holland, J.E., White, P.J., Glendining, M.J., Goulding, K.W.T., McGrath, S.P., 2019. Yield responses of arable crops to liming — an evaluation of relationships between yields and soil pH from a long-term liming experiment. Eur. J. Agron. 105, 176–188. https://doi.org/10.1016/j.eja.2019.02.016

Jouichat, H., Khiari, L., 2026. Reconstructing soil acidity neutralization curves using machine learning and chemical or spectral soil signatures. Geoderma 465, 117645. https://doi.org/10.1016/j.geoderma.2025.117645

Kouera, I., Khiari, L., 2026. Data-driven reconstruction of soil neutralization curves for lime requirement prediction in Sub-Saharan African soils. Geoderma 472, 117901. https://doi.org/10.1016/j.geoderma.2026.117901

Lavkulich, L.M., 1981. Methods Manual: Pedology Laboratory, 3rd printing. Department of Soil Science, University of British Columbia, Vancouver, BC.

Li, Y., Cui, S., Chang, S.X., Zhang, Q., 2019. Liming effects on soil pH and crop yield depend on lime material type, application method and rate, and crop species: a global meta-analysis. J. Soils Sediments 19, 1393–1406. https://doi.org/10.1007/s11368-018-2120-2

Lukin, V.V., Epplin, F.M., 2003. Optimal frequency and quantity of agricultural lime applications. Agric. Syst. 76, 949–967. https://doi.org/10.1016/S0308-521X(02)00016-1

Magdoff, F.R., Bartlett, R.J., 1985. Soil pH buffering revisited. Soil Sci. Soc. Am. J. 49, 145–148. https://doi.org/10.2136/sssaj1985.03615995004900010029x

Makaza, W., Khiari, L., El Achaby, M., 2026. The meta-analysis study on the effects of the quality of lime materials on the soil physicochemical properties and crop yields in acid soils. Front. Soil Sci. 6, 1725559. https://doi.org/10.3389/fsoil.2026.1725559

McLean, E.O., 1982. Soil pH and lime requirement, in: Page, A.L., Miller, R.H., Keeney, D.R. (Eds.), Methods of Soil Analysis, Part 2: Chemical and Microbiological Properties, 2nd ed. Agronomy Monograph 9. American Society of Agronomy and Soil Science Society of America, Madison, WI, pp. 199–224. https://doi.org/10.2134/agronmonogr9.2.2ed.c12

Meharg, A.A., Killham, K., 1990. The effect of soil pH on rhizosphere carbon flow of *Lolium perenne*. Plant Soil 123, 1–7. https://doi.org/10.1007/BF00009920

Mehlich, A., 1976. New buffer pH method for rapid estimation of exchangeable acidity and lime requirement of soils. Commun. Soil Sci. Plant Anal. 7, 637–652. https://doi.org/10.1080/00103627609366673

Mehlich, A., 1984. Mehlich 3 soil test extractant: a modification of Mehlich 2 extractant. Commun. Soil Sci. Plant Anal. 15, 1409–1416. https://doi.org/10.1080/00103628409367568

Mitscherlich, E.A., 1909. Das Gesetz des Minimums und das Gesetz des abnehmenden Bodenertrages. Landwirtsch. Jahrb. 38, 537–552.

Neina, D., 2019. The role of soil pH in plant nutrition and soil remediation. Appl. Environ. Soil Sci. 2019, 5794869. https://doi.org/10.1155/2019/5794869

Nelson, D.W., Sommers, L.E., 1982. Total carbon, organic carbon, and organic matter, in: Page, A.L., Miller, R.H., Keeney, D.R. (Eds.), Methods of Soil Analysis, Part 2: Chemical and Microbiological Properties, 2nd ed. Agronomy Monograph 9. American Society of Agronomy and Soil Science Society of America, Madison, WI, pp. 539–579. https://doi.org/10.2134/agronmonogr9.2.2ed.c29

OMAFRA, 2022. Agronomy Guide for Field Crops, Publication 811. Ontario Ministry of Agriculture, Food and Rural Affairs, Guelph, ON. https://www.ontario.ca/page/publication-811-agronomy-guide-field-crops (accessed 1 September 2026).

Parent, L.-E., Tremblay, C., 2002. Soil acidity determination methods for organic soils and peat materials, in: Parent, L.-E., Ilnicki, P. (Eds.), Organic Soils and Peat Materials for Sustainable Agriculture. CRC Press, Boca Raton, FL, pp. 93–104. https://doi.org/10.1201/9781420040098-5

Penn, C., Camberato, J., 2019. A critical review on soil chemical processes that control how soil pH affects phosphorus availability to plants. Agriculture 9, 120. https://doi.org/10.3390/agriculture9060120

Prasad, M., McDaniel, N., Kavanagh, A., Tzortzakis, N., 2021. Dolomitic lime rate effects on pH, available macro- and micro-nutrient content, plant growth and plant nutrient content on peats of various degrees of decomposition. Acta Hortic. 1305, 485–492. https://doi.org/10.17660/ActaHortic.2021.1305.64

Sebastià, J., van Oort, F., Lamy, I., 2008. Buffer capacity and Cu affinity of soil particulate organic matter (POM) size fractions. Eur. J. Soil Sci. 59, 304–314. https://doi.org/10.1111/j.1365-2389.2007.01001.x

Shoemaker, H.E., McLean, E.O., Pratt, P.F., 1961. Buffer methods for determining lime requirement of soils with appreciable amounts of extractable aluminum. Soil Sci. Soc. Am. J. 25, 274–277. https://doi.org/10.2136/sssaj1961.03615995002500040014x

Spillman, W.J., 1923. Application of the law of diminishing returns to some fertilizer and feed data. J. Farm Econ. 5, 36–52. https://doi.org/10.2307/1230266

Tang, C., Rengel, Z., 2003. Role of plant cation/anion uptake ratio in soil acidification, in: Rengel, Z. (Ed.), Handbook of Soil Acidity. Marcel Dekker, New York, pp. 57–81. https://doi.org/10.1201/9780203912317.ch3

Thomas, G.W., 1982. Exchangeable cations, in: Page, A.L., Miller, R.H., Keeney, D.R. (Eds.), Methods of Soil Analysis, Part 2: Chemical and Microbiological Properties, 2nd ed. Agronomy Monograph 9. American Society of Agronomy and Soil Science Society of America, Madison, WI, pp. 159–165. https://doi.org/10.2134/agronmonogr9.2.2ed.c9

Tran, T.S., van Lierop, W., 1982. Lime requirement determination for attaining pH 5.5 and 6.0 of coarse-textured soils using buffer-pH methods. Soil Sci. Soc. Am. J. 46, 1008–1014. https://doi.org/10.2136/sssaj1982.03615995004600050024x

van Lierop, W., 1981. Conversion of organic soil pH values measured in water, 0.01 M $CaCl_2$ or 1 N KCl. Can. J. Soil Sci. 61, 577–579. https://doi.org/10.4141/cjss81-067

van Lierop, W., 1983. Lime requirement determination of acid organic soils using buffer-pH methods. Can. J. Soil Sci. 63, 411–423. https://doi.org/10.4141/cjss83-043

Walkley, A., Black, I.A., 1934. An examination of the Degtjareff method for determining soil organic matter, and a proposed modification of the chromic acid titration method. Soil Sci. 37, 29–38. https://doi.org/10.1097/00010694-193401000-00003

Wilman, D., 1975. Nitrogen and Italian ryegrass. 1. Growth up to 14 weeks: dry-matter yield and digestibility. Grass Forage Sci. 30, 141–147. https://doi.org/10.1111/j.1365-2494.1975.tb01366.x

Xu, D., Zhu, Q., Ros, G., Cai, Z., Wen, S., Xu, M., Zhang, F., de Vries, W., 2022. Calculation of spatially explicit amounts and intervals of agricultural lime applications at county-level in China. Sci. Total Environ. 806, 150955. https://doi.org/10.1016/j.scitotenv.2021.150955

Figure captions

Fig. 1. Soil pH trajectories in clay, sandy loam and organic soil over five successive 12-week cropping cycles (C1–C5) following a single application of calcium carbonate ($CaCO_3$) at C0: the pretreatment baseline. Coloured lines represent $CaCO_3$ rates, the grey dashed line the unlimed control, the red dashed line the soil-specific target pH, and the shaded band the agronomic pH window.

Fig. 2. Cycle-specific Mitscherlich fits of the $CaCO_3$ dose response, with columns representing successive cropping cycles (C1–C5) and rows representing soils. Points are observed pH increments relative to the unlimed control of the same cycle (ΔpH) and solid curves are the fitted responses. Fitted parameters, the coefficient of determination (R^2) and the root mean square error (RMSE) are given in each panel.

Fig. 3. Evolution of the Mitscherlich parameters A and c across the five cropping cycles. Points with dashed connectors are the independently fitted cycle values shown with ±1 standard error, black lines are the functions selected by the corrected Akaike information criterion (AICc).

Fig. 4. Predicted versus observed pH for the curve-based analysis (blue circles) and the parametric surface (orange triangles) in clay, sandy loam and organic soil. Each symbol is one soil × rate × cycle observation and the dashed line is the 1:1 relationship. Predictions are compared with the observations used to fit the models; R^2 and RMSE are given above each panel.

Fig. 5. Curve-based and parametric $CaCO_3$ response surfaces for clay, sandy loam and organic soil. Colour and thin white isolines give fitted pH; the red dashed isoline is the target pH, the white dotted isolines are the agronomic bounds, and the red vertical line is the persistence-aware lime requirement $LR_{freq}(N_{max})$.

Fig. 6. Predicted pH trajectories at selected $CaCO_3$ rates from the curve-based analysis and the parametric surface (lower row), with each rate labelled in the panel legend. LR_{peak} is the smallest rate reaching the target pH, $LR_{freq}(N_{max})$ the persistence-aware rate over N_{max} cycles, $D_{min}(5)$ the smallest rate holding pH above the lower bound through C5, D_{max} the largest rate within the upper bound, and LR_{CRAAQ} the regional Centre de référence en agriculture et agroalimentaire du

Québec (CRAAQ) rate. The black dashed line is the target pH and the shaded band the agronomic pH window. N_{max} is two cycles in sandy loam and five in the other soils.

Fig. 7. First fitted cycle with pH below the lower agronomic limit as a function of the $CaCO_3$ rate, in clay, sandy loam and organic soil. The staircase is solid at rates up to D_{max}, the largest rate within the upper bound, and dashed beyond it, where the grey band marks rates exceeding the upper limit in at least one cycle. Vertical lines mark LR_{peak}, the smallest rate reaching the target pH; $LR_{freq}(N_{max})$, the persistence-aware rate; and, in sandy loam, $D_{min}(5)$, the smallest rate holding pH above the lower bound through C5. "No crossing through C5" denotes rates that never fell below the lower limit.

Fig. 8. Five-cycle feasible dose corridor as a function of the width of the agronomic pH window (δ), with each soil's lower:upper margin ratio held constant as δ was varied. The corridor lies between $D_{min}(5)$ (red dashed), the smallest rate holding pH above the lower bound through C5, and D_{max} (dark dash-dot), the largest rate within the upper bound; the thick red line is $LR_{freq}(5)$, the persistence-aware rate over five cycles. Dotted segments indicate closed corridors, the × marks the smallest δ at which the corridor opens, and the grey vertical line the δ used for the primary calculations.

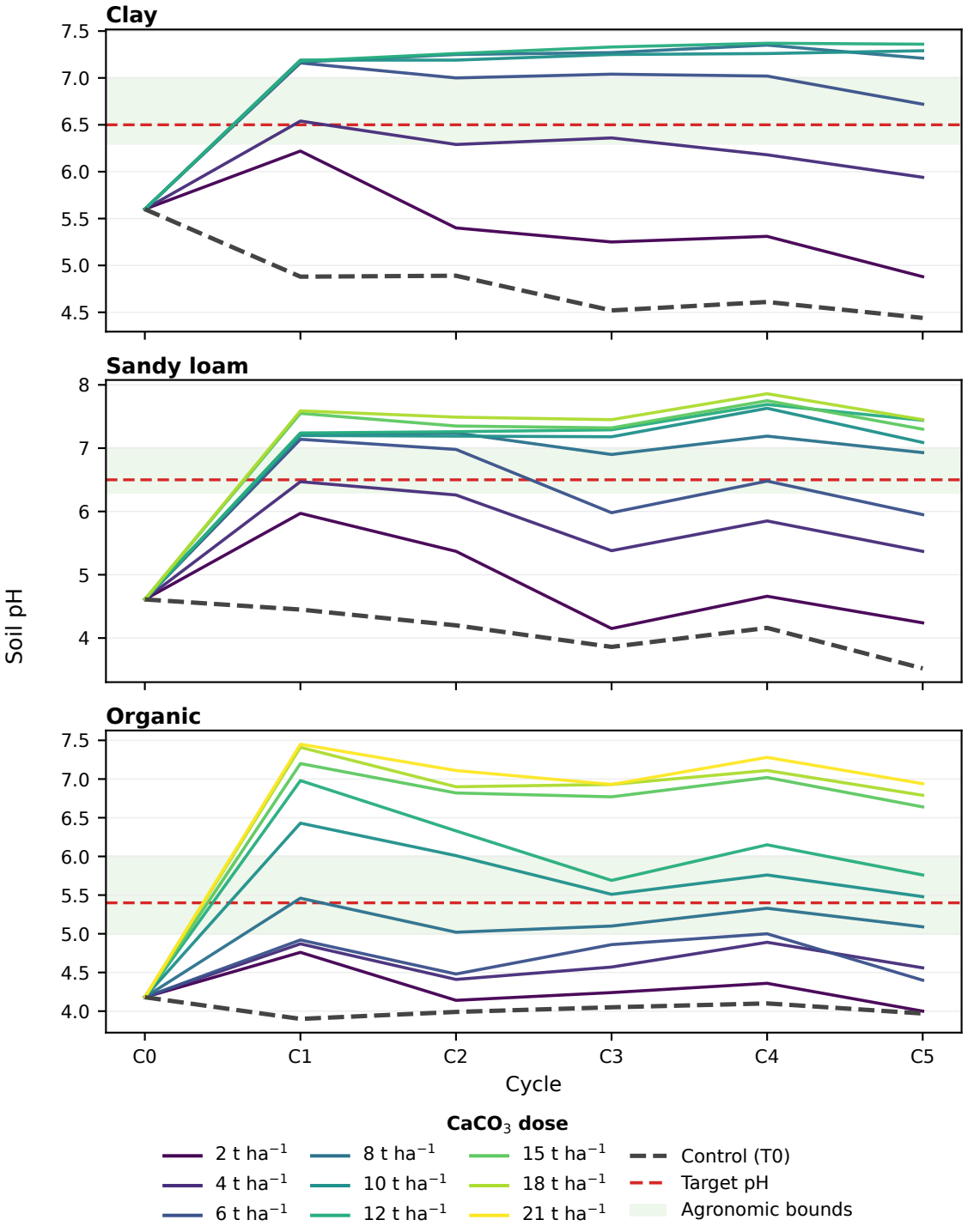
Clay
Sandy loam
Organic
Soil pH
Cycle
C0
C1
C2
C3
C4
C5
CaCO3 dose
2 t ha−1
4 t ha−1
6 t ha−1
8 t ha−1
10 t ha−1
12 t ha−1
15 t ha−1
18 t ha−1
21 t ha−1
Control (T0)
Target pH
Agronomic bounds

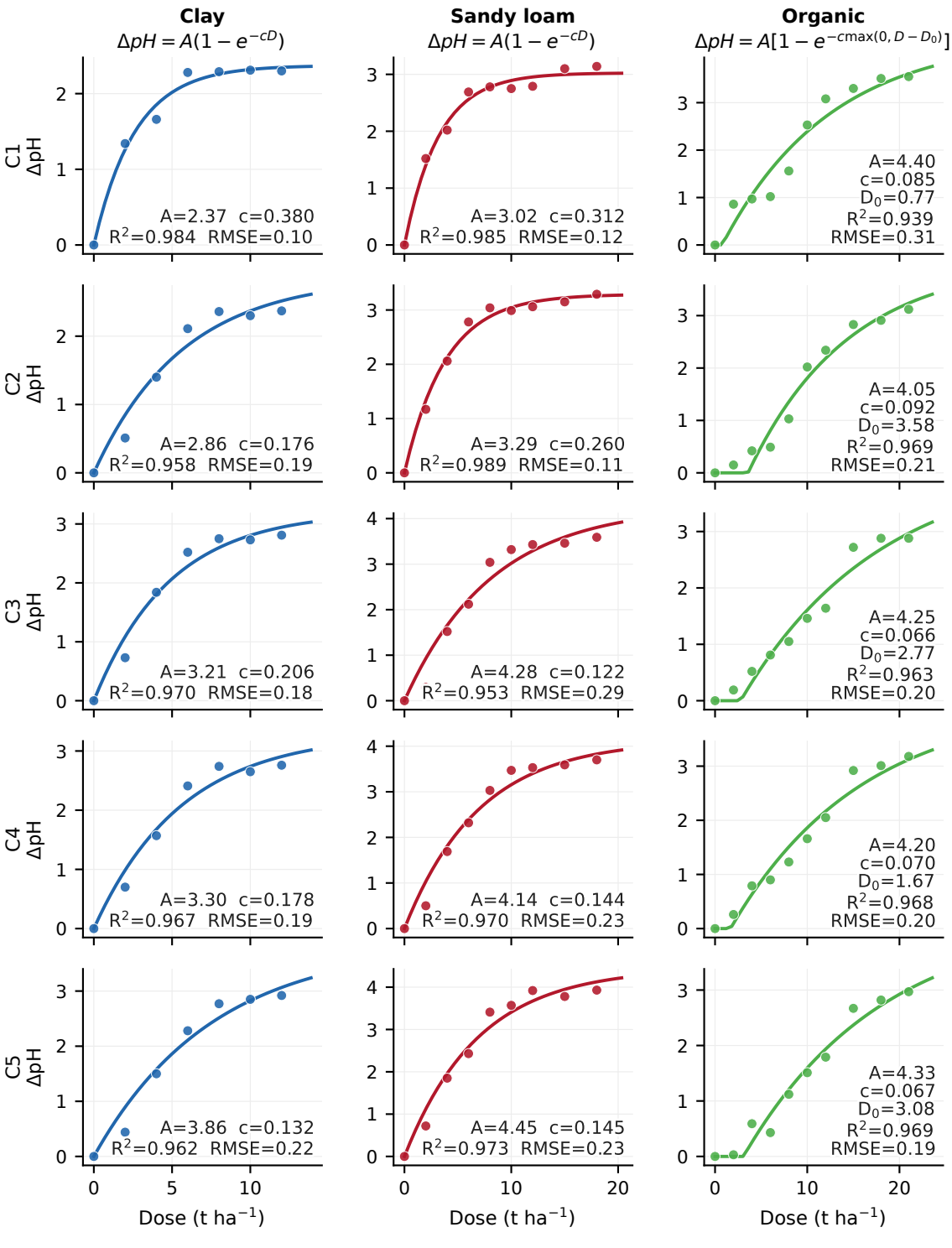
Clay
$\Delta pH = A(1 - e^{-cD})$
Sandy loam
$\Delta pH = A(1 - e^{-cD})$
Organic
$\Delta pH = A[1 - e^{-c\max(0, D - D_0)}]$
C1 ΔpH
C2 ΔpH
C3 ΔpH
C4 ΔpH
C5 ΔpH
A=2.37 c=0.380
R²=0.984 RMSE=0.10
A=3.02 c=0.312
R²=0.985 RMSE=0.12
A=4.40
c=0.085
D₀=0.77
R²=0.939
RMSE=0.31
A=2.86 c=0.176
R²=0.958 RMSE=0.19
A=3.29 c=0.260
R²=0.989 RMSE=0.11
A=4.05
c=0.092
D₀=3.58
R²=0.969
RMSE=0.21
A=3.21 c=0.206
R²=0.970 RMSE=0.18
A=4.28 c=0.122
R²=0.953 RMSE=0.29
A=4.25
c=0.066
D₀=2.77
R²=0.963
RMSE=0.20
A=3.30 c=0.178
R²=0.967 RMSE=0.19
A=4.14 c=0.144
R²=0.970 RMSE=0.23
A=4.20
c=0.070
D₀=1.67
R²=0.968
RMSE=0.20
A=3.86 c=0.132
R²=0.962 RMSE=0.22
A=4.45 c=0.145
R²=0.973 RMSE=0.23
A=4.33
c=0.067
D₀=3.08
R²=0.969
RMSE=0.19
Dose (t ha⁻¹)
Dose (t ha⁻¹)
Dose (t ha⁻¹)

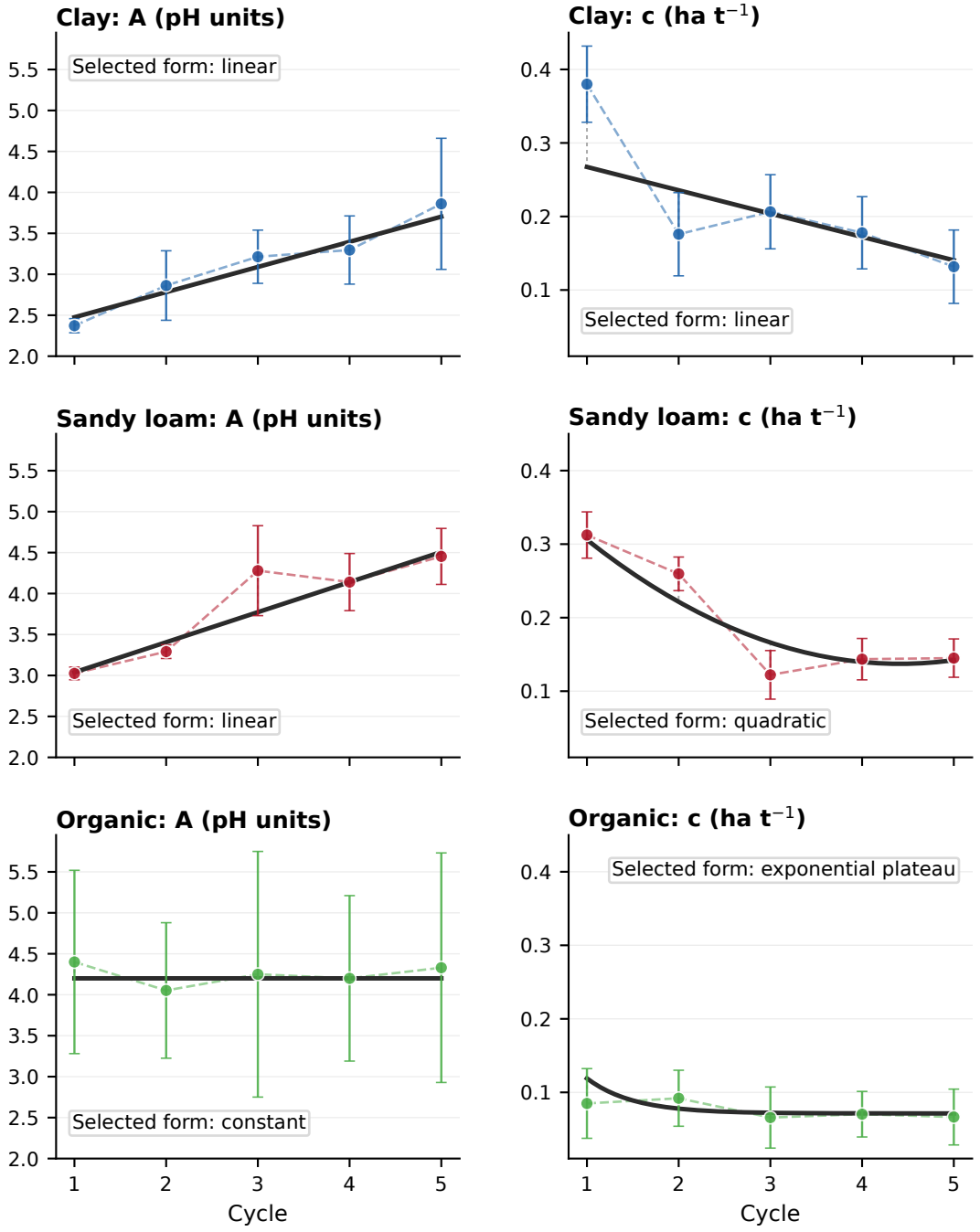
Clay: A (pH units)
Selected form: linear
Clay: c (ha t^{-1})
Selected form: linear
Sandy loam: A (pH units)
Selected form: linear
Sandy loam: c (ha t^{-1})
Selected form: quadratic
Organic: A (pH units)
Selected form: constant
Organic: c (ha t^{-1})
Selected form: exponential plateau
Cycle
Cycle

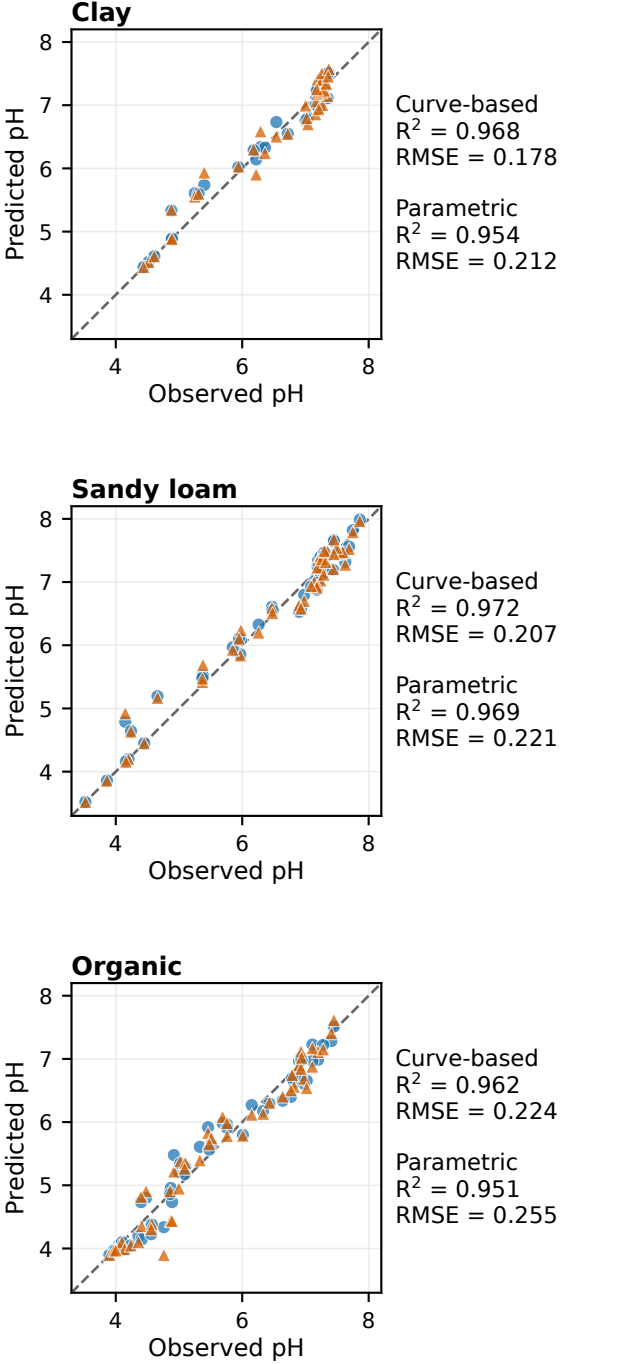
Clay
Predicted pH
Observed pH
Curve-based
R² = 0.968
RMSE = 0.178
Parametric
R² = 0.954
RMSE = 0.212
Sandy loam
Predicted pH
Observed pH
Curve-based
R² = 0.972
RMSE = 0.207
Parametric
R² = 0.969
RMSE = 0.221
Organic
Predicted pH
Observed pH
Curve-based
R² = 0.962
RMSE = 0.224
Parametric
R² = 0.951
RMSE = 0.255
1:1 line
Curve-based
Parametric

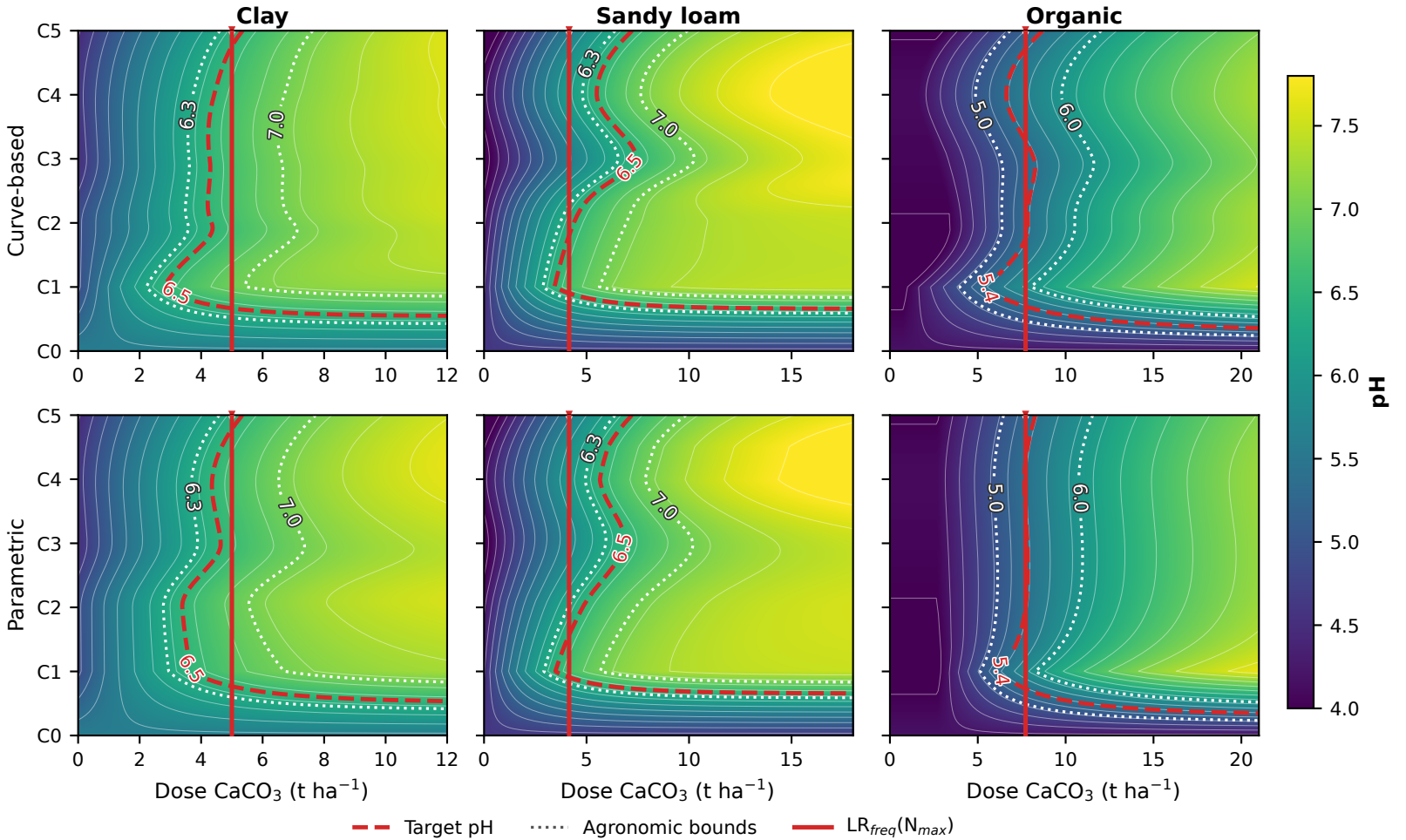
Clay
Sandy loam
Organic
Curve-based
Parametric
C5
C4
C3
C2
C1
C0
0
2
4
6
8
10
12
15
20
6.3
6.5
7.0
5.0
5.4
6.0
Dose CaCO3 (t ha−1)
pH
7.5
7.0
6.5
6.0
5.5
5.0
4.5
4.0
Target pH
Agronomic bounds
LRfreq(Nmax)

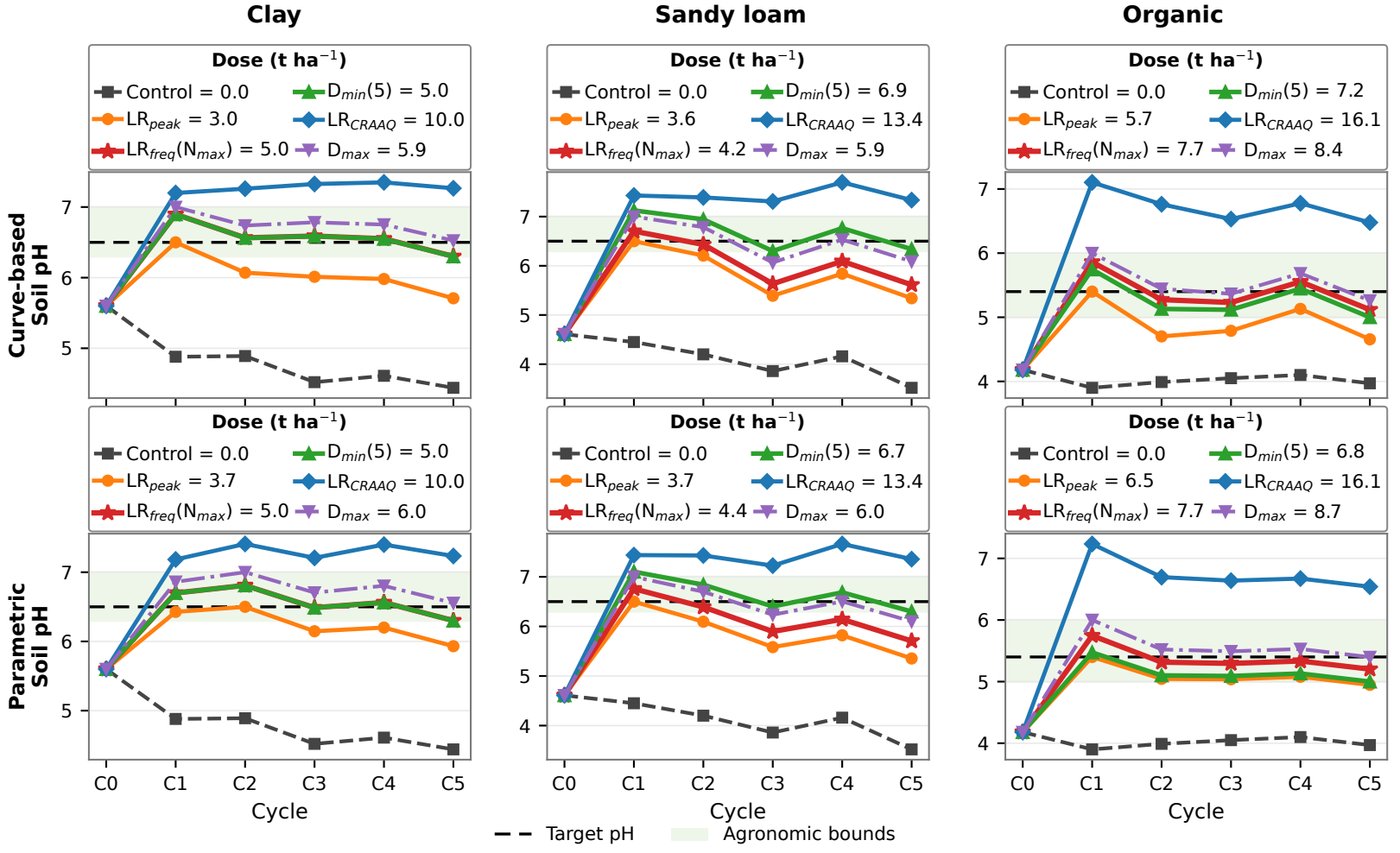
Clay
Sandy loam
Organic
Curve-based Soil pH
Parametric Soil pH
Dose (t ha^{-1})
Control = 0.0
D_{min}(5) = 5.0
LR_{peak} = 3.0
LR_{CRAAQ} = 10.0
$LR_{freq}(N_{max})$ = 5.0
D_{max} = 5.9
D_{min}(5) = 6.9
LR_{peak} = 3.6
LR_{CRAAQ} = 13.4
$LR_{freq}(N_{max})$ = 4.2
D_{max} = 5.9
D_{min}(5) = 7.2
LR_{peak} = 5.7
LR_{CRAAQ} = 16.1
$LR_{freq}(N_{max})$ = 7.7
D_{max} = 8.4
D_{min}(5) = 5.0
LR_{peak} = 3.7
LR_{CRAAQ} = 10.0
$LR_{freq}(N_{max})$ = 5.0
D_{max} = 6.0
D_{min}(5) = 6.7
LR_{peak} = 3.7
LR_{CRAAQ} = 13.4
$LR_{freq}(N_{max})$ = 4.4
D_{max} = 6.0
D_{min}(5) = 6.8
LR_{peak} = 6.5
LR_{CRAAQ} = 16.1
$LR_{freq}(N_{max})$ = 7.7
D_{max} = 8.7
C0 C1 C2 C3 C4 C5
Cycle
Target pH
Agronomic bounds

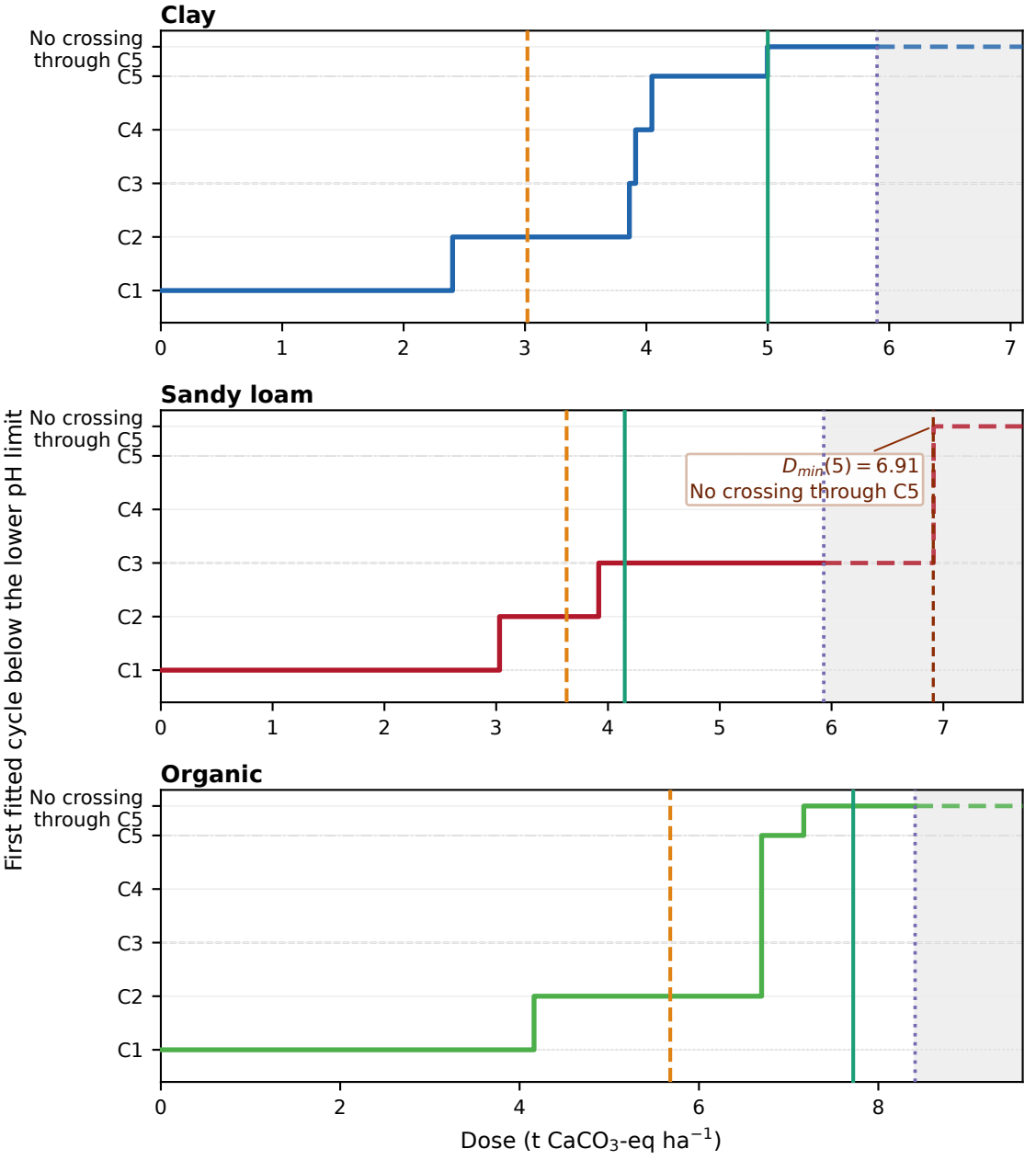
Clay
Sandy loam
Organic
No crossing through C5
C5
C4
C3
C2
C1
First fitted cycle below the lower pH limit
$D_{min}(5) = 6.91$
No crossing through C5
0
1
2
3
4
5
6
7
8
Dose (t $CaCO_3$-eq ha^{-1})
LR_{peak}
$LR_{freq}(N_{max})$
D_{max}
$D > D_{max}$ (upper-bound excursion)

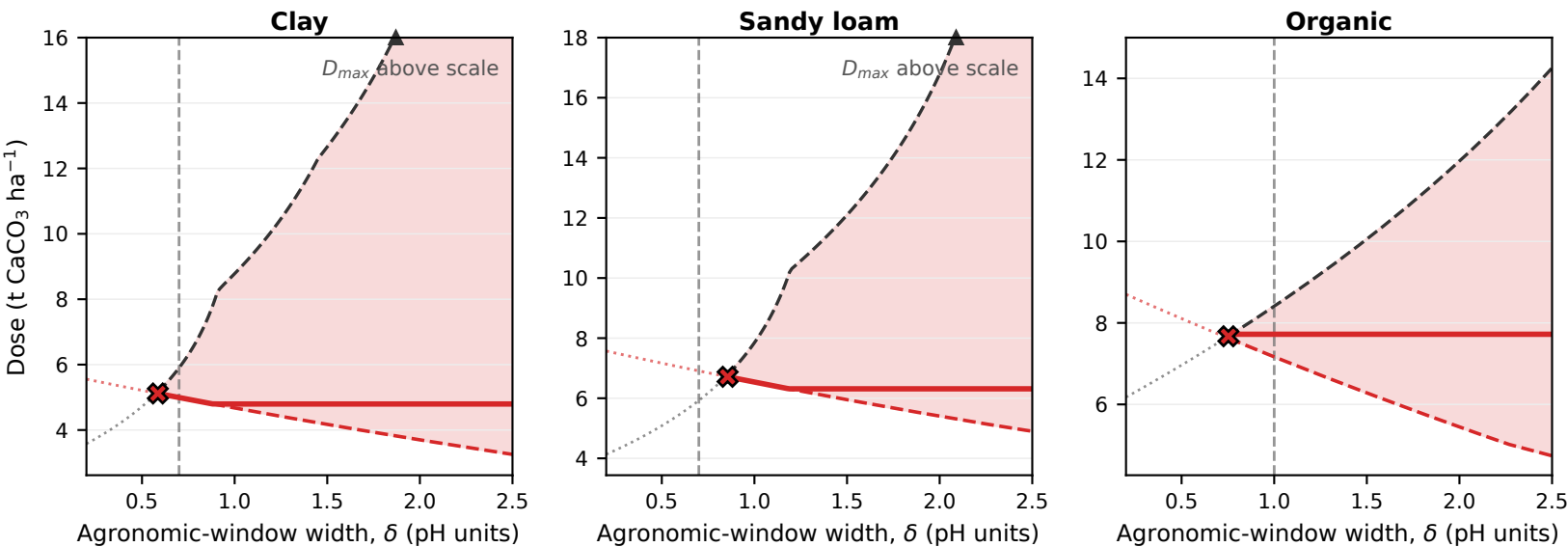
Clay
Sandy loam
Organic
D_{max} above scale
D_{max} above scale
Dose (t $CaCO_3$ ha^{-1})
Agronomic-window width, δ (pH units)
Agronomic-window width, δ (pH units)
Agronomic-window width, δ (pH units)
Feasible N = 5 corridor
D_{max}
Smallest feasible δ
$D_{min}(5)$
$LR_{freq}(5)$
Canonical δ

Supplementary material

$CaCO_3$ was the primary liming material used to develop the rate–frequency framework. CaO was analysed as a secondary comparison after conversion to $CaCO_3$-equivalent dose. This supplement presents the CaO biomass results, lime-requirement metrics, selected parametric functions, and response surfaces cited in the manuscript. Fig. S2 summarises model selection for the primary $CaCO_3$ parametric surface.

Supplementary tables

Table S1. Ryegrass dry mass and Spearman correlation with CaO application rate by soil and cycle.

Cycle	Soil	Mean DM ± SD (g pot^{-1})	CV (%)	ρ
1	Clay	6.51 ± 0.93	14.3	−0.29
1	Sandy loam	3.82 ± 1.26	33.1	−0.73
1	Organic	4.23 ± 1.35	31.8	+0.73
2	Clay	5.75 ± 0.55	9.5	+1.00
2	Sandy loam	5.30 ± 0.79	14.8	−0.07
2	Organic	4.58 ± 2.03	44.3	+0.89
3	Clay	5.70 ± 0.68	11.9	+0.50
3	Sandy loam	6.94 ± 1.04	14.9	−0.15
3	Organic	8.56 ± 1.84	21.5	+0.47
4	Clay	5.73 ± 0.35	6.1	+0.39
4	Sandy loam	4.83 ± 0.81	16.7	−0.37
4	Organic	4.61 ± 1.49	32.3	+0.93
5	Clay	5.88 ± 0.29	5.0	+0.32
5	Sandy loam	5.01 ± 0.81	16.3	−0.07
5	Organic	5.38 ± 1.49	27.7	+0.82

Note: DM = dry mass; SD = standard deviation; CV = coefficient of variation; ρ = Spearman correlation between applied CaO dose and per-cycle DM. DM is the per-pot sum of three harvests within each 12-week cycle. Mean ± SD, CV and ρ were calculated across all tested CaO rates: seven rates for clay (0–6.72 t ha^{-1}), nine for sandy loam (0–10.08 t ha^{-1}) and ten for organic soil (0–11.76 t ha^{-1}), corresponding to 0–12, 0–18 and 0–21 t $CaCO_3$-equivalent ha^{-1}. Each treatment was represented by one pot.

Table S2. CaO rate–frequency and peak-response metrics from the curve-based analysis and parametric surface.

Metric	Clay		Sandy loam		Organic	
	Curve-based	Parametric	Curve-based	Parametric	Curve-based	Parametric
LR_{CRAAQ}	10.00	10.00	13.40	13.40	16.10	16.10
N_{max}	5	5	2	2	5	5
LR_{peak}	4.76	5.61	5.03	4.86	7.71	7.98
$LR_{freq}(N_{max})$	6.47	6.22	5.58	6.07	9.89	9.47
$r(N_{max})$	1.36	1.11	1.11	1.25	1.28	1.19
$D_{min}(5)$	6.47	5.95	9.99	9.85	9.28	8.33
D_{max}	7.30	8.46	7.52	7.30	10.19	10.30

Note: Rates are expressed as t $CaCO_3$-equivalent ha^{-1}, and C1–C5 denote five successive 12-week cropping cycles. Curve-based values were obtained from the five independently fitted cycle curves and parametric values from the AICc-selected functions of cycle. LR_{CRAAQ} is the regional SMP-buffer estimate made before the experiment. N_{max} is the greatest number of consecutive cycles for which at least one dose remained between the lower and upper pH limits. LR_{peak} is the smallest dose whose highest fitted pH across C1–C5 reached the target. $LR_{freq}(N_{max})$ is the feasible dose with the smallest mean squared deviation from target pH over that horizon. $r(N_{max}) = LR_{freq}(N_{max})/LR_{peak}$. $D_{min}(5)$ is the smallest dose that remained at or above the lower pH limit through C5. D_{max} is the largest dose that remained at or below the upper pH limit throughout C1–C5.

Table S3. Selected parametric functions of cycle and fit metrics for the CaO surface.

Soil	A(t)	c(t)	$D_0(t)$	k	R^2	RMSE	$\Delta AICc_{next}$
Clay	3.780	0.114	–	2	0.928	0.226	0.38
Sandy loam	3.059 + 0.339t	$0.083 + (0.300 - 0.083)e^{-0.703t}$	–	5	0.943	0.259	0.37
Organic	4.405	$0.060 + (1.707 - 0.060)e^{-3.724t}$	3.794	5	0.926	0.297	0.99

Note: Dose is expressed as t $CaCO_3$-equivalent ha^{-1} and t is the 12-week cycle index. A(t) is the fitted maximum pH increase above the unlimed control, approached as dose increases; c(t) controls the curvature of that response across dose; and $D_0(t)$ is the dose threshold below which no lime-induced pH increase is assigned. An en dash indicates that no threshold was fitted, as for the mineral soils. k is the number of fitted coefficients. R^2 and RMSE describe agreement with all observed pH values, with RMSE in pH units. $\Delta AICc_{next}$ is the difference in AICc from the next-ranked candidate, where AICc is the Akaike information criterion corrected for small sample size. Coefficients are rounded to three decimals.

Supplementary figure captions

Fig. S1. Curve-based and parametric CaO response surfaces for clay, sandy loam and organic soil, with CaO expressed as $CaCO_3$ equivalent. Colour and thin white isolines give fitted pH; the red dashed isoline is the target pH, the white dotted isolines are the agronomic bounds, and the red vertical line is the persistence-aware lime requirement $LR_{freq}(N_{max})$. Selected parametric functions are given in Table S3.

Fig. S2. Corrected Akaike information criterion (AICc) comparison of candidate parameter-evolution combinations within the parametric $CaCO_3$ surface, for clay, sandy loam and organic soil. Candidate labels give the functional forms in the order A(t) / c(t) for the mineral soils and A(t) / c(t) / D_0(t) for the organic soil. Bars show ΔAICc relative to the best candidate within a soil, which is marked with a diamond at ΔAICc = 0, and k is the number of fitted coefficients.

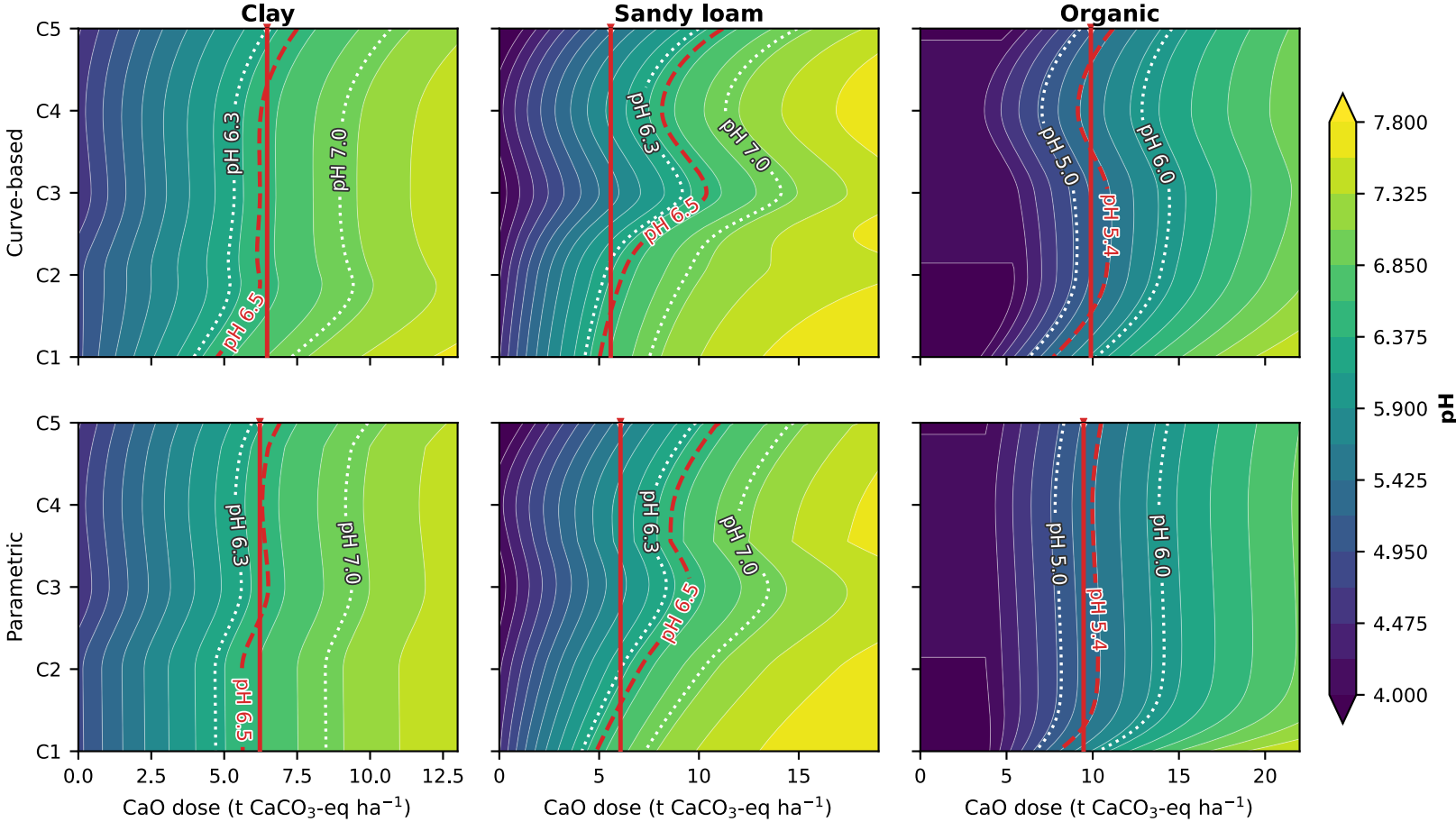
Clay
Sandy loam
Organic
Curve-based
Parametric
C5
C4
C3
C2
C1
pH 6.3
pH 6.5
pH 7.0
pH 5.0
pH 5.4
pH 6.0
0.0
2.5
5.0
7.5
10.0
12.5
0
5
10
15
20
CaO dose (t CaCO3-eq ha−1)
pH
7.800
7.325
6.850
6.375
5.900
5.425
4.950
4.475
4.000
Target pH
Agronomic bounds
LRfreq(Nmax)

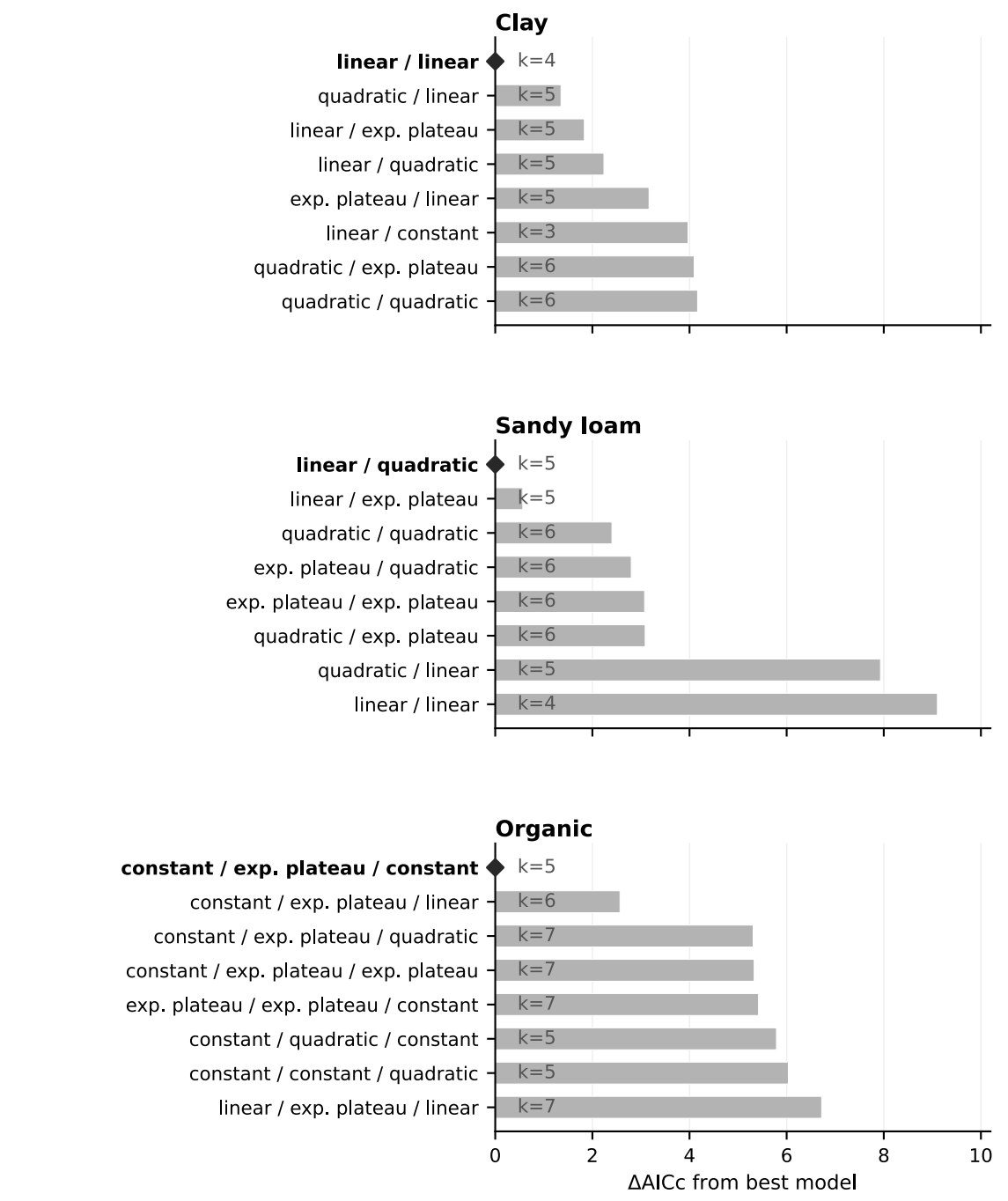
Clay
linear / linear
quadratic / linear
linear / exp. plateau
linear / quadratic
exp. plateau / linear
linear / constant
quadratic / exp. plateau
quadratic / quadratic
k=4
k=5
k=5
k=5
k=5
k=3
k=6
k=6
Sandy loam
linear / quadratic
linear / exp. plateau
quadratic / quadratic
exp. plateau / quadratic
exp. plateau / exp. plateau
quadratic / exp. plateau
quadratic / linear
linear / linear
k=5
k=5
k=6
k=6
k=6
k=6
k=5
k=4
Organic
constant / exp. plateau / constant
constant / exp. plateau / linear
constant / exp. plateau / quadratic
constant / exp. plateau / exp. plateau
exp. plateau / exp. plateau / constant
constant / quadratic / constant
constant / constant / quadratic
linear / exp. plateau / linear
k=5
k=6
k=7
k=7
k=7
k=5
k=5
k=7
0
2
4
6
8
10
ΔAICc from best model